Received: 18 March 2022 | Revised: 17 June 2022 | Accepted: 30 June 2022

DOI: 10.1111/geb.13569

Global Ecology and Biogeography — A Journal of Macroecology

WILEY

RESEARCH ARTICLE

Pyrogeography across the western Palaearctic: A diversity of fire regimes

Juli G. Pausas

CIDE-CSIC, Consejo Superior de Investigaciones Científicas, Valencia, Spain

Correspondence
Juli G. Pausas, CIDE-CSIC, Consejo Superior de Investigaciones Científicas, ES-46113 Montcada, Valencia, Spain.
Email: juli.g.pausas@ext.uv.es; juli.g.pausas@csic.es

Funding information
European Commission, Grant/Award Number: GA 101003890

Handling Editor: Morgan Varner

Abstract

Aim: The aim was to characterize fire regimes and estimate fire regime parameters (area burnt, size, intensity, season, patchiness and pyrodiversity) at broad spatial scales using remotely sensed individual-fire data.

Location: Western part of the Palaearctic realm (i.e., Europe, North Africa and the Near East).

Time period: 2001–2021.

Methods: Initially, I divided the study area into eight large ecoregions based on their environment and vegetation: Mediterranean, Arid, Atlantic, Mountains, Boreal, Steppes, Continental and Tundra. Next, I intersected each predefined ecoregion with individual-fire data obtained from remote sensing hotspots to estimate fire regime parameters for each environment. This allowed me to compute annual area burnt, fire size, fire intensity, fire season, fire patchiness, fire recurrence and pyrodiversity for each ecoregion. I related those fire parameters to the climate of the ecoregions and analysed the temporal trends in fire size.

Results: Fire regime parameters varied across different environments (ecoregions). The Mediterranean had the largest, most intense and most recurrent fires, but the Steppes had the largest burnt area. Arid ecosystems had the most extended fire season, Tundra had the patchiest fires, and Boreal forests had the earliest fires of the year. The spatial variability in fire regimes was largely explained by the variability of climate and vegetation, with a tendency for greater fire activity in the warmer ecoregions. There was also a temporal tendency for large fires to become larger during the last two decades, especially in Arid and Continental environments.

Main conclusion: The fire regime characteristics of each ecoregion are unique, with a tendency for greater fire activity in warmer environments. In addition, fires have been increasing in size during recent decades.

KEYWORDS
Europe, fire regime, fire–climate, Near East, North Africa

1 | INTRODUCTION

Fire regimes are shaped by climate, landscape structure and the frequency of ignitions (Pausas & Keeley, 2021) and vary globally across space, biogeographies and environments (Archibald et al., 2013; Bradstock, 2010; Chuvieco et al., 2008, 2021; Dennison et al., 2014; Krawchuk et al., 2009; Pausas & Ribeiro, 2013; van der Werf et al., 2008). This variability in fire regimes selects for distinct species traits (Keeley et al., 2011; Keeley & Zedler, 1998), structures the assembly of communities (Pausas & Ribeiro, 2017; Ponisio et al., 2016; Sauquet et al., 2009; Verdú & Pausas, 2007) and determines biome distributions (Bond et al., 2005; Pausas & Bond, 2020). Fire regimes are also strongly sensitive to human activities (Archibald, 2016; Balch et al., 2017; Pausas & Fernández-Muñoz, 2012; Syphard et al., 2017) and global change drivers (Abram et al., 2021; Hanes et al., 2019; Pausas & Keeley, 2021; Westerling et al., 2006), and the changes in fire regime have strong effects on ecosystems, biodiversity (Kelly et al., 2020; Mahood & Balch, 2019) and societies (Reisen et al., 2015). Fire regimes are therefore a key factor for understanding many past and future ecological patterns. However, we lack knowledge on fire regimes for many world regions because data on wildfires have not always been recorded and published systematically. This might be because in many regions, fires were not sufficiently important to justify establishing a fire agency, or because political instability precluded the existence of such agencies. This data gap limits our understanding of the effects of global change on fire regimes at broad scales. Remotely sensed data can, to some extent, fill this gap, because there are satellites detecting thermal anomalies across the entire globe (hotspots; Giglio et al., 2006). In fact, remotely sensed fire data have provided a novel view of fire across the world by showing us its ubiquity (the fire overview effect; i.e., similar to the awareness by astronauts when viewing the entire Earth during space flight).

Now that we have a couple of decades of remotely sensed fire data, we can start to understand fire regimes at broad spatial scales. By fire regime, we refer to the variations in a diversity of fire parameters (e.g., size, intensity, recurrence, seasonality and patchiness) that characterize the occurrence of fires in each region. Although remotely sensed data have limitations (Schroeder et al., 2008; van der Werf et al., 2008), such data provide a standardized way to compare regions (and periods) where ground information is scarce or uneven (e.g., across different countries). These data can also be useful for describing current fire regimes and detecting future fire regime shifts, which are especially relevant in our changing world. The question is, to what extent do remotely sensed fire data depict fire regime variability for estimation of fire regime parameters?

Previous research on remotely sensed fire data has focused mostly on grid-cell (pixel-scale) analysis of fire regimes (Archibald et al., 2013; Chuvieco et al., 2008) and classified those pixels into a handful of groups describing global syndromes of fire regimes (pyromes; Archibald et al., 2013). The use of arbitrary grid cells has limitations (spatial autocorrelation; van der Werf et al., 2008), and the results are difficult to incorporate into ecological and management problems. Analyses based on ecological regions (ecoregions) might be more appropriate for many biological questions (Smith et al., 2018), including fire regimes (Erni et al., 2020; Hanes et al., 2019; Syphard & Keeley, 2020), because fires are strongly related to vegetation (fuel) and climate, and these factors are key for the definition of ecoregions. However, in most cases, previous region-based analyses have used point data for fires (MODIS hotspots; e.g., Pausas & Ribeiro, 2013, 2017), and these data do not capture useful fire regime characteristics fully and make it difficult to estimate fire regime parameters.

To improve our understanding of fire regimes at broad scales, I consider various environmentally homogeneous areas with broad vegetation types, and I benefit from the recent development of data based on individual fires (fire scars; Andela et al., 2019; Artés et al., 2019; Laurent et al., 2018, 2019). A regional fire scars approach (instead of hotspots and grid cells) should provide more ecologically meaningful information on fire regimes (i.e., at the ecological and biogeographical scale) and enable regional patterns to be found that can later be related to other regional processes (e.g., species and biome distribution). Such an approach is also more aligned with ground-based statistics and management concepts (e.g., fire size, fire recurrence) and more useful for modelling purposes. Adopting this approach, I aim to compare and estimate fire regime parameters for different ecoregions with different environmental conditions, different dominant vegetation (biomes) and different biogeographical origins. I also aim to determine whether there is any temporal tendency for some of the fire regime parameters during the last decades. Although human activities diminish the importance of these factors for fire regimes (Archibald, 2016; Balch et al., 2017; Chergui et al., 2018; Pausas & Fernández-Muñoz, 2012; Syphard et al., 2017), I propose that at broad scales, the interactions among vegetation, climate and fire are still relevant even in highly populated areas. I hypothesize that different environmentally defined regions (hereafter, ecoregions) have distinct fire regimes. I predict that in temperate environments, warm ecosystems will tend to be more flammable than cold ones, and that there will be a tendency towards increasing fire size.

Specifically, I test this approach in the western part of the Palaearctic realm; this is a large biogeographical unit that includes Europe, North Africa and the Near East (Figure 1), comprising 78 countries and encompassing most major temperate ecosystems. This area includes regions with high and low population densities, regions that are fire-prone and others traditionally considered non-fire-prone, and regions with ineffective policies. These differences make field fire information data unavailable or spatially heterogeneous. I use large regions with different environmental conditions and dominant vegetations (ecoregions; Figure 1a) to study variation in the fire regime across the western Palaearctic, including temporal trends in fire size for each of the ecoregions. Although fires in the European Mediterranean area are relatively well known, our knowledge of other Palaearctic regions is fragmentary (e.g., Belhadj-Khedher et al., 2020; Chergui et al., 2018; Curt et al., 2020; Dubinin et al., 2011).

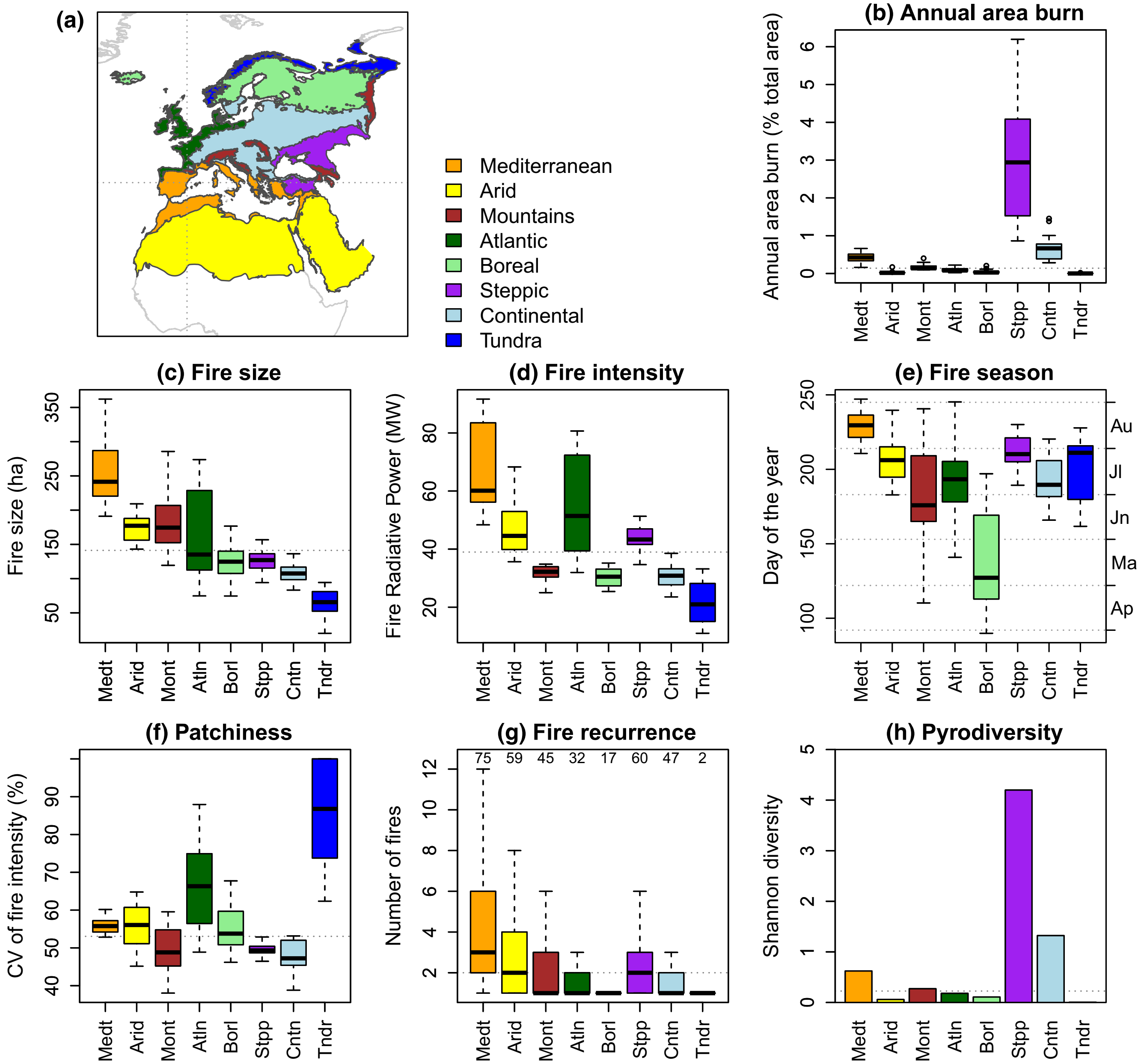

FIGURE 1 (a) Map of the study area (dotted lines indicate latitude 40 and longitude 0), with the eight ecoregions indicated in different colours (the same colours are used for the other figures). (b) Proportion of the area burnt annually (as a percentage). (c) Mean fire size (in hectares). (d) Mean fire intensity (fire radiactive power, in megawatts in 1 km pixels). (e) Fire season (mean of the day of the year that fires start; dotted horizontal lines separate different months). (f) Patchiness of the fire intensity for each fire. (g) Fire recurrence as number of fires in each fire patch (boxplot) and as the proportion of fire patches with more than one fire (numbers at the top). (h) Pyrodiversity (diversity of fire patches). Details of the ecoregions and data are given in the Supporting Information (Tables S1 and S2). Boxplots reflect variability over the years and include the median (horizontal line), the first and third quartiles (box) and extreme values (excluding outliers). Dotted lines refer to the median value across ecoregions, except for panel (a), where they indicate latitude = 40, longitude = 0, and panel (e), where they separate months. A summary of all this information is provided in the ordination of Figure 2. See also the Supporting Information (Figures S1–S11).

2 | METHODS

2.1 | Ecoregions

The study region is the western part of Palaearctic Realm; it includes 78 countries (21,896,929 km^2) of Europe (52% of the area), North Africa (30%) and the Near East (18%). In this extensive area, I defined the following eight environmental regions (ecoregions): Mediterranean, Arid, Atlantic, Mountains, Boreal, Steppes, Continental and Tundra (Figure 1a; for details see Supporting Information Tables S1 and S2; Figure S1). The use of large ecoregions enables the estimation of some fire parameters with relatively few years of data. These ecoregions are defined by aggregating 81 World Wide Fund for Nature (WWF) ecoregions (Dinerstein et al., 2017; Supporting Information Table S1) with the help of the bioregions (https://www.oneearth.org/bioregions-2020). The eight ecoregions differ in their climates, dominant vegetation (biome) and biogeographical origin. The use of these ecoregions reduces the spatial autocorrelation problems faced by studies using grid cells, while providing useful fire regime information at an ecological and biogeographical scale. The Arid region is the largest (*c.* 10.5×10^6 km^2), followed by Continental (*c.* 3.4×10^6 km^2), Boreal (2.2×10^6 km^2), Mediterranean (2×10^6 km^2), Steppes (1.5×10^6 km^2), Atlantic (0.9×10^6 km^2), Mountains (0.7×10^6 km^2) and Tundra (0.6×10^6 km^2; Supporting Information Table S1).

2.2 | Data

To estimate fire regime parameters in each ecoregion, I considered the three available databases that include the geolocated individual fires across the globe: GlobFire (Artés et al., 2019), FRY (Laurent et al., 2018, 2019) and FireAtlas (Andela et al., 2019). These databases were prepared using different algorithms and assumptions, as described in the references; they also differ slightly in the period considered (Supporting Information Table S3). GlobFire is the most recently published and has the most years of data. It also includes a comparison with precedents and validations with independent data, and considerable agreement was found among the databases (see also Galizia et al., 2021), but some biases in the precedents were also found (e.g., the problem of using tildes that split fires in FireAtlas). In addition, GlobFire provides the perimeter of all fires in a GIS format, enabling me to study fire overlaps (hence recurrence and pyrodiversity; see below). However, GlobFire and FireAtlas do not have any indicators of fire intensity. Therefore, my analysis for size-based statistics is based on GlobFire, whereas for fire intensity statistics, I rely on FRY and on direct remotely sensed data (MODIS hotspots; Collection 6 Active Fire Products from Terra and Aqua satellites, dataset MCD14ML; spatial resolution: 1 km; downloaded from the University of Maryland, USA; period 2001–2021; Supporting Information Table S3). Note that the latter data (MODIS fire intensity) are at pixel scale (not for individual fires). To ensure that my results do not depend on the data set used, I repeated the same analyses with alternative data sets (results shown in Figure S2–S11 of the Supporting Information). For a general characterization of the ecoregions, I use climate data from WorldClim v.2.1 (Fick & Hijmans, 2017).

2.3 | Analysis

Remotely sensed fire data are prone to false positives because they are based on thermal anomalies. To reduce these false positives, I initially applied a mask on all the fire databases using a map of potential false positives that included petrochemical industry centres (e.g., Algeria and Persian Gulf), volcanoes (e.g., Iceland and Etna) and highly industrialized centres. Each fire/hotspot was then assigned to an ecoregion by intersecting its geolocation with the ecoregion map. I computed the following fire statistics for each ecoregion and year (sources for each parameter are in Supporting Information Table S3): number of fires; area burnt; fire size; fire intensity; fire season; duration of the fire season; and fire patchiness (coefficient of variation of the fire intensity in each fire). For fire size and intensity, I also computed the maximum values as the 95th percentile (Archibald et al., 2013). The data were then averaged by ecoregion and year and displayed by ecoregion using boxplots (with the median and percentiles across years). GlobFire data enabled me to compute the overlap between fires throughout the study period and to study the different fire-produced patches in the landscape. Fire recurrence for each ecoregion was estimated as the number of times each patch was burnt. The pyrodiversity of each ecoregion (i.e., fire-caused landscape heterogeneity; Martin & Sapsis, 1992, He et al., 2019) was estimated as the Shannon diversity of fire patches; that is, considering the relative abundance (sizes) of fire-produced patches in each ecoregion.

Ecoregion mean values for fire parameters were summarized with a principal components analysis (PCA) using the R *stats* library, with variables centred and scaled. Ecoregion means were also regressed against average climate variables using generalized additive (smoothing) models as implemented in the R package "`mgcv`" (Wood, 2017). I tested precipitation and temperature variables for annual averages and for the driest and wettest quarter of the year following WorldClim data.

Skewness (asymmetry) and Pearson's kurtosis ("tailedness") of the fire size and fire intensity distribution for the whole study area and for each ecoregion were computed using the R package "`moments`". The relationship between fire size and intensity was analysed for FRY data (the only data set that had both variables) using generalized additive models ("`mgcv`" R package). To check whether there was a temporal trend in the extreme fire activity, I regressed fire size against time using 95% quantile regression as implemented in the R package "`quantreg`" (Koenker, 2021). The previously published pyrome map (Archibald et al., 2013) has relatively poor information for much of the study area, but I overlaid it with my ecoregions to check whether my results were consistent with the pyrome map.

3 | RESULTS

During the last two decades, fire has been omnipresent in most of the western Palaearctic. Fire occurred across all ecoregions and, except for the Tundra, it occurred every year; however, there were conspicuous differences in fire regime among ecoregions (Figures 1 and 2). Steppes and Continental areas were the areas with the highest number of fires (Supporting Information Figure S2); considering the size of the ecoregion, Steppes had the largest proportion of annual area burnt, followed by Continental and Mediterranean (Figure 1b;

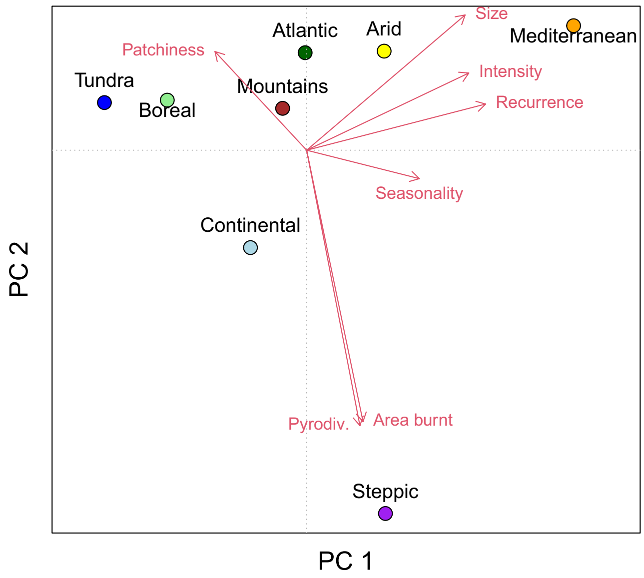

FIGURE 2 Principal components analysis of seven fire characteristics (area burnt, seasonality, fire recurrence, fire intensity, fire size, patchiness and pyrodiversity) across the eight ecoregions (for details, see Figure 1). The first axis (PC 1) accounts for 43.6% of the variability, and the second (PC 2) for 32%; that is, the two-dimensional space accounts for 75.6% of the variability.

Supporting Information Figures S3 and S4). However, fires in Steppes and Continental ecoregions were relatively small and of low intensity when compared with the Mediterranean ecoregion, which had the largest and most intense fires (Figures 1c,d and 2; Supporting Information Figures S5–S8). European boreal fires were of relatively low intensity (Figures 1d and 2). The smallest and least intense fires occurred in the Tundra, where fires were very patchy (Figures 1c,d,f and 2; Supporting Information Figure S8). Boreal fires mostly occurred in spring or early summer; Mediterranean fires peaked in August, and fires peaked in July for the other ecoregions (Figure 1e; Supporting Information Figure S9). July was the month with most fires across the whole region. The longest fire seasons were observed in Arid and Mountains, and the shortest in Tundra and Boreal ecoregions (Supporting Information Figure S10). During the period with fire data (*c.* 18 years; Supporting Information Table S3), fires were frequent enough to overlap, especially in the Mediterranean, and to lesser extent in Arid and Steppes ecoregions; and this generated a landscape with patches recurrently burned (Figure 1g). Landscape pyrodiversity (Figure 1h) showed a similar pattern across ecoregions for the number of fires (Supporting Information Figure S2) and area burnt (Figures 1b and 2), with the highest pyrodiversity in Steppes, followed by Continental and Mediterranean ecoregions. Average fire size, fire intensity and fire recurrence tended to increase towards warmer ecoregions, whereas fire patchiness tended to be greater in cold ecoregions (Figure 3; Supporting Information Table S4).

For all ecoregions, fire size distributions and fire intensity distributions were positively skewed, with long tails (Table 1; Supporting Information Figures S12–S14); that is, the larger and the more intense the fires, the rarer they were. Skewness and kurtosis were correlated across ecoregions for both fire size and fire intensity ($r = 0.96$, $t = 8.68$, d.f. = 6, $p < .01$ and $r = 0.98$, $t = 11.89$, d.f. = 6, $p < .0001$, respectively; i.e., the greater the distribution asymmetry, the longer the tail). Fire size was much more skewed than fire intensity (Table 1; Supporting Information Table S5); the most skewed distribution was for Continental, followed by Steppe and Boreal; Tundra was the least skewed. The consequence of this strong skewness with high kurtosis was that the largest 1% of fires accounted for 30% of the area burnt (over the entire study region; Table 1; Supporting Information Figure S15). This value varied across ecoregions (Table 1; Supporting Information Figure S12), being highest in the Mediterranean (34.2%) and lowest for Tundra (16%). Fire size and fire intensity were positively correlated (Supporting Information Figure S16), suggesting that high-intensity fires propagate faster and tend to generate larger fires (Laurent et al., 2019). Despite the relatively short temporal window considered, there is a significant tendency for large fires to increase in size, especially in Arid and Continental environments (Table 1).

The pyrome map (Archibald et al., 2013) has no information for Tundra and little information for Arid, Atlantic, Boreal and Mountains, yet it tends to agree with the present results (Supporting Information Figure S17 compared with Figure 1). For instance, the dominant pyrome for Atlantic, Boreal and Mountains was RCS (rare-cool-small fires), which is consistent with the present results (Figures 1 and 2). It is also consistent with the fact that the area with most pixels with rare-intense-large fires was the Mediterranean, the area with most pixels with frequent-cool-small fires was the Steppes, and fires in the Continental area were small and cool (intermediate-cool-small, RCS) (Supporting Information Figure S17).

4 | DISCUSSION

Wildfires are currently common across all the western Palaearctic. The Mediterranean ecoregion is where the fires are the largest, most intense and most recurrent, as can be expected given the considerable fire activity in this ecoregion each summer (Keeley et al., 2012; also evidenced in headlines of newspapers). However, fires are not limited to this ecoregion (Figures 1 and 2). For instance, the Steppes (e.g., the Pontic steppes) is the ecoregion where fires are most numerous and occupy the largest proportion of the landscape, despite being small and of low intensity, and it is also the area with the greatest temperature seasonality (Supporting Information Table S2). The Steppes evolved with large herbivores that are now extinct or drastically reduced in number (e.g., Librado et al., 2021; Zimov et al., 1995), hence fires are likely to be replacing them as an alternative biomass consumer (Bond & Keeley, 2005; Pausas & Bond, 2020). Therefore, including large herbivores (rewilding or livestock) would seem appropriate for fuel management in these steppes. Tundra, in contrast, is the ecosystem with least fire activity, and when fires occur they are the patchiest. Tundra ecosystems are especially sensitive to increased fire activity owing to climate warming and the subsequent

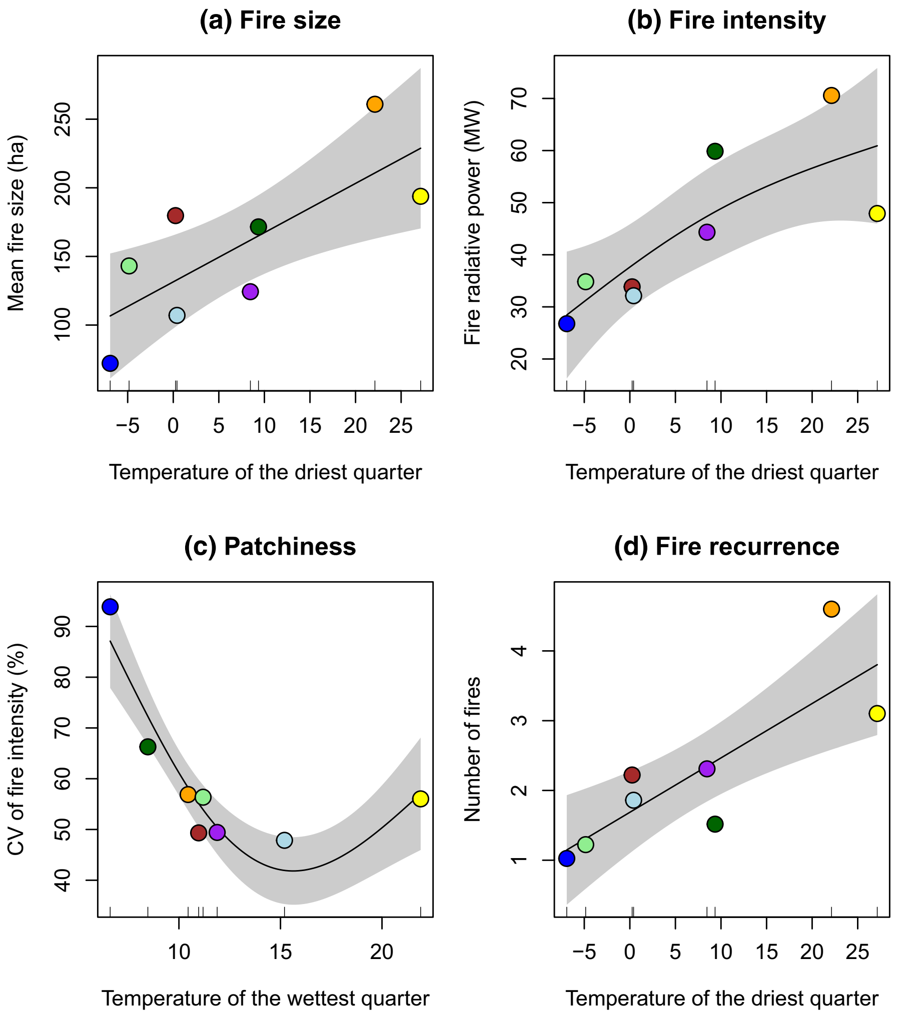

FIGURE 3 Relationship between fire regime parameter (*y*-axes) and average climate characteristics (*x*-axes) across ecoregion (colours; see Figure 1). Climate parameters are mean temperatures (in degrees Celsius) of the driest quarter (a, b, d) and the wettest quarter (c). The lines are significant ($p < .05$) smoothing regressions (generalized additive model) with confidence intervals (shading). For details of the statistical models, see the Supporting Information (Table S4). CV, coefficient of variation.

shrub cover expansion and ice shrinkage (Hu et al., 2010). European boreal fires are of relatively low intensity (Figure 1d), which is consistent with field observations in the Eurasian boreal forest (e.g., understorey and litter-fuelled fires; Sannikov & Goldammer, 1996; Kharuk et al., 2021) and in contrast to American boreal fires, as has been observed previously (Archibald et al., 2018; Rogers et al., 2015). Palaearctic fires are strongly seasonal (Figure 1e), and this emphasizes the importance of weather conditions for fire.

Overall, fire regimes are diverse across the study area (Figure 1), and each ecoregion is unique in its fire characteristics (Figure 2), with an increasing fire activity in warmer ecoregions (Figure 3). These results suggest that at the broad scale, summer temperature is a good indicator of ecosystem flammability in temperate environments (Figure 2), with the Mediterranean showing higher than expected fire activity for its temperature (positive residuals in Figure 2), and the Arid ecoregion (the warmest) showing lower than expected fire activity (negative residuals). This deviation from expectation is likely to be explained by fuel, with heavy fuels in Mediterranean shrublands and sparse fuels in Arid ecosystems. These results also highlight the sensitivity of temperate ecosystems to changes in summer temperatures (Pausas & Paula, 2012). Certainly, there is also variability within ecoregion, not only because of the variability in climate and topography, but also because of the diversity of socioeconomic factors (e.g., European vs. African Mediterranean ecoregions; Chergui et al., 2018), yet the present results suggest that there are strong constraints imposed by climate and vegetation. In other words, human factors are important in shaping fire regimes (Andela et al., 2017; Archibald, 2016; Balch et al., 2017; Cattau et al., 2020; Chergui et al., 2018; Pausas & Fernández-Muñoz, 2012; Syphard et al., 2017), but at broad scales they are unlikely to be the main driver differentiating ecoregions.

The present results are consistent across fire databases (Supporting Information Figures S2–S11) and with global pyromes (Archibald et al., 2013), and they provide finer-scale information on fire regimes. Aggregating fire data on climatically homogeneous ecoregions allows the estimation of some fire parameters that are difficult to estimate when aggregating small pixels in fragmented pyromes. This is important when the temporal window is relatively short, because large areas have more information for understanding fire regimes. The drawback of the ecoregion approach is that some areas might be heterogeneous in vegetation and fire parameters, thus both approaches might be complementary. The simple fire regime classifications most typically used (i.e., low-intensity surface fires vs. high-intensity crown fires) have been very useful

TABLE 1 Skewness and Pearson's kurtosis of the fire size and fire intensity distributions, in addition to temporal trends in large fires (in hectares), for the eight environments considered (Figure 1; Supporting Information Figures S12 and S13) and for the overall western Palaearctic (Supporting Information Figure S15)

	Fire size distribution			Fire intensity distribution		Temporal trend in fire size	
Ecoregion	Skewness	Kurtosis	%AB	Skewness	Kurtosis	*F*	Coefficient
Mediterranean	42.1	2,872.3	**34.2**	10.5	180.3	1.37	−8.40
Arid	35.2	2,046.3	31.4	11.3	240.1	33.28***	55.02***
Mountains	31.7	1,875.8	26.6	14.3	392.4	0.63	−12.77
Atlantic	19.7	657.6	27.1	8.4	125.2	1.17	24.11
Boreal	80.1	7,298.6	33.9	**16.8**	**554.6**	0.58	13.25
Steppes	146.2	31,694.5	32.7	8.2	131.5	1.25	2.02
Continental	**230.8**	**81,391.3**	21.3	12.3	380.9	163.49***	21.40***
Tundra	6.4	58.1	16.2	4.3	28.3	1.14	0.12
Overall	149.7	35,961.2	30.0	14.7	419.5	163.06***	15.99***

Notes: %AB refers to the proportion of area burnt by the largest 1% of fires. The temporal trend is computed as the 95% quantile regressions for each environment considered; the columns are the *F*-values and the coefficient of the regressions. Fire size is based on GlobFire (Artés et al., 2019) and fire intensity in the MODIS hotspots (aqua) (for alternative data sources, see Supporting Information Table S3). Bold values indicate the ecoregion with the highest value for the corresponding column.

***There was a significant increase in large fires ($p < .0001$).

as a primary axis of variation for understanding fire adaptive traits (Keeley et al., 2011; Keeley & Zedler, 1998; Pausas, 2015). The present finer-scale differences in fire regime among ecoregions open the opportunity for a deeper analysis of the relationship between fire regimes and the distribution of species, traits and biomes.

Despite the relatively short temporal scale considered, I detected a significant overall tendency for large fires to increase in size, and this tendency was driven mainly by the Arid and Continental environments (Table 1). This is consistent with the general perception of increasingly frequent large fires in the region and with observations in other regions (e.g., Dennison et al., 2014). This is important because fire size is often related to the severity of the fire and to the postfire regeneration, because the recolonization capacity of fire-sensitive species might increase with fire size (García et al., 2016; Owen et al., 2017); this is not considered when using annual area burnt. In addition, fire size is sensitive to fire management and societal factors (Pausas & Fernández-Muñoz, 2012; Piñol et al., 2005), which might also be unnoticed or confounded with an increasing number of fires when studying annual area burnt instead of individual fires. In fact, it is possible to have a declining tendency in the number of fires and area burned (Andela et al., 2017; Marlon et al., 2008) but an increasing size of fires, which might reflect an increase in extreme fires. And this is the expectation when firefighting resources and abilities are increasing but conditions (climate, weather and fuels) are becoming more conducive to fire. Overall, the present results suggest that to account better for the variability in fire regimes and their impact, it is important to consider a diversity of dimensions of fire regime that can be estimated using individual fire scars. This should also enable us to gain a better understanding of future regime shifts (i.e., shifts in any of the fire dimensions).

Remotely sensed data come with limitations for estimating fire regimes; these include: (1) a short time window, which might preclude finding clear differences across regions; (2) the variety of sources, algorithms and assumptions, which might make results inconsistent; and (3) light understorey fires and underground fires might go unnoticed by remote sensors (Schroeder et al., 2008). The short time window limits our ability to understand the frequency of fires and the long-term regime. This limitation is, in part, compensated by the large size of the ecoregions considered, and the present results show clear and expected differences across environments. In the future, this limitation will be even more relaxed. In relationship to the different sources, I evaluated fire regime parameters from a range of sources (Supporting Information Table S3), and the results were consistent, suggesting that this is not a key issue, at least at the scale of the present study (see also Artés et al., 2019; Galizia et al., 2021). Small fires are likely to be underrepresented (Galizia et al., 2021), but they are also the least important. Finally, remote sensing data are likely to fail to capture underground (peat) fires that occur mainly in Tundra (Turetsky et al., 2011), hence this type of fire needs to be added to the present results to gain a full understanding of fires in this ecoregion. However, the great patchiness of tundra fires (Figure 1) suggests that, to some extent, it might be depicting a range of fire types. In any case, the intensity of peat fires might be defined better by the depth they reach than by the above-ground radiation captured remotely. The low fire intensity of some forest biomes (e.g., Boreal and Mountain) suggests that remotely sensed data might be depicting understorey fires. Despite many limitations, the analysis of individual fires based on remotely sensed data enables us to study fire regimes at broad spatial scales that cannot otherwise be achieved, hence it becomes an essential tool for ecological studies.

Fires are sensitive to climate, increased urban population in wildlands and changes in land use (Pausas & Keeley, 2021). In a business-as-usual scenario, the continuous abandonment of many rural landscapes across the Palaearctic, climate change and the tendency for increasing human activities in the wild (e.g., the spread of the wildland–urban interface) have established the appropriate conditions for increasing the frequency of large fires. To what extent we will deviate from this path is unknown; it will depend on our own decisions. Monitoring changes in fire activity using individual fires in the different regions might provide us with a realistic picture of the trends and shifts of fire regime at broad spatial scales.

ACKNOWLEDGMENTS

I thank E. Ribeiro, A. Descals and A. Verger for their help in the GIS analysis, S. Archibald for providing the pyrome map in a workable format, and M. Varner for helpful suggestions. This work was inspired by meetings of the FIRELink Cost Action (European Commission CA18135) and performed under the framework of the fireUrisk project (European Commission GA 101003890; European Union's Horizon 2020 research and innovation programme).

DATA AVAILABILITY STATEMENT

All data was obtained from published references or public repositories, as indicated in the Methods section and in Table S3. The map (Fig. 1a) and the aggregated data are openly available in DRYAD at https://doi.org/10.5061/dryad.k98sf7m8c

ORCID

Juli G. Pausas https://orcid.org/0000-0003-3533-5786

TWITTER

Juli G. Pausas @jgpausas

REFERENCES

Abram, N. J., Henley, B. J., Sen Gupta, A., Lippmann, T. J. R., Clarke, H., Dowdy, A. J., Sharples, J. J., Nolan, R. H., Zhang, T., Wooster, M. J., Wurtzel, J. B., Meissner, K. J., Pitman, A. J., Ukkola, A. M., Murphy, B. P., Tapper, N. J., & Boer, M. M. (2021). Connections of climate change and variability to large and extreme forest fires in Southeast Australia. *Communications Earth & Environment*, *2*, 1–17.

Andela, N., Morton, D. C., Giglio, L., Chen, Y., van der Werf, G. R., Kasibhatla, P. S., DeFries, R. S., Collatz, G. J., Hantson, S., Kloster, S., Bachelet, D., Forrest, M., Lasslop, G., Li, F., Mangeon, S., Melton, J. R., Yue, C., & Randerson, J. T. (2017). A human-driven decline in global burned area. *Science*, *356*, 1356–1362.

Andela, N., Morton, D. C., Giglio, L., Paugam, R., Chen, Y., Hantson, S., van der Werf, G. R., & Randerson, J. T. (2019). The global fire atlas of individual fire size, duration, speed and direction. *Earth System Science Data*, *11*, 529–552.

Archibald, S. (2016). Managing the human component of fire regimes: Lessons from Africa. *Philosophical Transactions of the Royal Society of London B: Biological Sciences*, *371*, 20150346.

Archibald, S., Lehmann, C. E. R., Belcher, C. M., Bond, W. J., Bradstock, R. A., Daniau, A.-L., Dexter, K. G., Forrestel, E. J., Greve, M., He, T., Higgins, S. I., Hoffmann, W. A., Lamont, B. B., McGlinn, D. J., Moncrieff, G. R., Osborne, C. P., Pausas, J. G., Price, O., Ripley, B. S., … Zanne, A. E. (2018). Biological and geophysical feedbacks with fire in the Earth system. *Environmental Research Letters*, *13*, 033003

Archibald, S., Lehmann, C. E. R., Gómez-Dans, J. L., & Bradstock, R. A. (2013). Defining pyromes and global syndromes of fire regimes. *Proceedings of the National Academy of Sciences USA*, *110*, 6442–6447.

Artés, T., Oom, D., de Rigo, D., Durrant, T. H., Maianti, P., Libertà, G., & San-Miguel-Ayanz, J. (2019). A global wildfire dataset for the analysis of fire regimes and fire behaviour. *Scientific Data*, *6*, 296.

Balch, J. K., Bradley, B. A., Abatzoglou, J. T., Nagy, R. C., Fusco, E. J., & Mahood, A. L. (2017). Human-started wildfires expand the fire niche across the United States. *Proceedings of the National Academy of Sciences USA*, *114*, 2946–2951.

Belhadj-Khedher, C., Ei-Melki, T., & Mouillot, F. (2020). Saharan hot and dry sirocco winds drive extreme fire events in mediterranean Tunisia (North Africa). *Atmosphere*, *11*, 590.

Bond, W. J., & Keeley, J. E. (2005). Fire as a global "herbivore": The ecology and evolution of flammable ecosystems. *Trends in Ecology & Evolution*, *20*, 387–394.

Bond, W. J., Woodward, F. I., & Midgley, G. F. (2005). The global distribution of ecosystems in a world without fire. *New Phytologist*, *165*, 525–538.

Bradstock, R. A. (2010). A biogeographic model of fire regimes in Australia: Current and future implications. *Global Ecology and Biogeography*, *19*, 145–158.

Cattau, M. E., Wessman, C., Mahood, A., & Balch, J. K. (2020). Anthropogenic and lightning-started fires are becoming larger and more frequent over a longer season length in the USA. *Global Ecology and Biogeography*, *29*, 668–681.

Chergui, B., Fahd, S., Santos, X., & Pausas, J. G. (2018). Socioeconomics drive fire regime variability in the Mediterranean Basin. *Ecosystems*, *21*, 619–628.

Chuvieco, E., Giglio, L., & Justice, C. (2008). Global characterization of fire activity: Toward defining fire regimes from earth observation data. *Global Change Biology*, *14*, 1488–1502.

Chuvieco, E., Pettinari, M. L., Koutsias, N., Forkel, M., Hantson, S., & Turco, M. (2021). Human and climate drivers of global biomass burning variability. *Science of the Total Environment*, *779*, 146361.

Curt, T., Aini, A., & Dupire, S. (2020). Fire activity in Mediterranean forests (the Algerian case). *Fire*, *3*, 58.

Dennison, P. E., Brewer, S. C., Arnold, J. D., & Moritz, M. A. (2014). Large wildfire trends in the western United States, 1984–2011. *Geophysical Research Letters*, *41*, 2928–2933.

Dinerstein, E., Olson, D., Joshi, A., Vynne, C., Burgess, N. D., Wikramanayake, E., Hahn, N., Palminteri, S., Hedao, P., Noss, R., Hansen, M., Locke, H., Ellis, E. C., Jones, B., Barber, C. V., Hayes, R., Kormos, C., Martin, V., Crist, E., … Saleem, M. (2017). An ecoregion-based approach to protecting half the terrestrial realm. *Bioscience*, *67*, 534–545.

Dubinin, M., Luschekina, A., & Radeloff, V. C. (2011). Climate, livestock, and vegetation: What drives fire increase in the arid ecosystems of southern Russia? *Ecosystems*, *14*, 547–562.

Erni, S., Wang, X., Taylor, S., Boulanger, Y., Swystun, T., Flannigan, M., & Parisien, M.-A. (2020). Developing a two-level fire regime zonation system for Canada. *Canadian Journal of Forest Research*, *50*, 259–273.

Fick, S. E., & Hijmans, R. J. (2017). WorldClim 2: New 1-km spatial resolution climate surfaces for global land areas. *International Journal of Climatology*, *37*, 4302–4315.

Galizia, L. F., Curt, T., Barbero, R., & Rodrigues, M. (2021). Assessing the accuracy of remotely sensed fire datasets across the southwestern Mediterranean Basin. *Natural Hazards and Earth System Sciences*, *21*, 73–86.

García, Y., Castellanos, M. C., & Pausas, J. G. (2016). Fires can benefit plants by disrupting antagonistic interactions. *Oecologia*, *182*, 1165–1173.

Giglio, L., Csiszar, I., & Justice, C. O. (2006). Global distribution and seasonality of active fires as observed with the Terra and Aqua moderate resolution imaging spectroradiometer (MODIS) sensors. *Journal of Geophysical Research*, *111*, G02016.

Hanes, C. C., Wang, X., Jain, P., Parisien, M.-A., Little, J. M., & Flannigan, M. D. (2019). Fire-regime changes in Canada over the last half century. *Canadian Journal of Forest Research*, *49*, 256–269.

He, T., Lamont, B. B., & Pausas, J. G. (2019). Fire as a key driver of Earth's biodiversity. *Biological Reviews*, *94*, 1983–2010.

Hu, F. S., Higuera, P. E., Walsh, J. E., Chapman, W. L., Duffy, P. A., Brubaker, L. B., & Chipman, M. L. (2010). Tundra burning in Alaska: Linkages to climatic change and sea ice retreat. *Journal of Geophysical Research*, *115*(G4), 2009JG001270.

Keeley, J. E., Bond, W. J., Bradstock, R. A., Pausas, J. G., & Rundel, P. W. (2012). *Fire in Mediterranean ecosystems: Ecology, evolution and management*. Cambridge University Press.

Keeley, J. E., Pausas, J. G., Rundel, P. W., Bond, W. J., & Bradstock, R. A. (2011). Fire as an evolutionary pressure shaping plant traits. *Trends in Plant Science*, *16*, 406–411.

Keeley, J. E., & Zedler, P. H. (1998). Evolution of life histories in Pinus. In D. M. Richardson (Ed.), *Ecology and biogeography of Pinus* (pp. 219–250). Cambridge University Press.

Kelly, L. T., Giljohann, K. M., Duane, A., Aquilué, N., Archibald, S., Batllori, E., Bennett, A. F., Buckland, S. T., Canelles, Q., Clarke, M. F., Fortin, M.-J., Hermoso, V., Herrando, S., Keane, R. E., Lake, F. K., McCarthy, M. A., Morán-Ordóñez, A., Parr, C. L., Pausas, J. G., … Brotons, L. (2020). Fire and biodiversity in the Anthropocene. *Science*, *370*, eabb0355.

Kharuk, V. I., Ponomarev, E. I., Ivanova, G. A., Dvinskaya, M. L., Coogan, S. C. P., & Flannigan, M. D. (2021). Wildfires in the Siberian taiga. *Ambio*, *50*, 1953–1974.

Koenker, R. (2021). *quantreg: Quantile regression*. R package version 5.86. https://cran.r-project.org/package=quantreg

Krawchuk, M. A., Moritz, M. A., Parisien, M.-A., Van Dorn, J., & Hayhoe, K. (2009). Global Pyrogeography: The current and future distribution of wildfire. *PLoS One*, *4*, e5102.

Laurent, P., Mouillot, F., Moreno, M. V., Yue, C., & Ciais, P. (2019). Varying relationships between fire radiative power and fire size at a global scale. *Biogeosciences*, *16*, 275–288.

Laurent, P., Mouillot, F., Yue, C., Ciais, P., Moreno, M. V., & Nogueira, J. M. P. (2018). FRY, a global database of fire patch functional traits derived from space-borne burned area products. *Scientific Data*, *5*, 180132.

Librado, P., Khan, N., Fages, A., Kusliy, M. A., Suchan, T., Tonasso-Calvière, L., Schiavinato, S., Alioglu, D., Fromentier, A., Perdereau, A., Aury, J.-M., Gaunitz, C., Chauvey, L., Seguin-Orlando, A., Der Sarkissian, C., Southon, J., Shapiro, B., Tishkin, A. A., Kovalev, A. A., … Orlando, L. (2021). The origins and spread of domestic horses from the Western Eurasian steppes. *Nature*, *598*, 634–640.

Mahood, A. L., & Balch, J. K. (2019). Repeated fires reduce plant diversity in low-elevation Wyoming big sagebrush ecosystems (1984–2014). *Ecosphere*, *10*, e02591.

Marlon, J. R., Bartlein, P. J., Carcaillet, C., Gavin, D. G., Harrison, S. P., Higuera, P. E., Joos, F., Power, M. J., & Prentice, I. C. (2008). Climate and human influences on global biomass burning over the past two millennia. *Nature Geoscience*, *1*, 697–702.

Martin, R. E., & Sapsis, D. B. (1992). Fires as agents of biodiversity: Pyrodiversity promotes biodiversity. In H. M. Kerner (Ed.), *Proceedings of the conference on biodiversity of Northwest California, 1991* (pp. 150–157). University of California.

Owen, S. M., Sieg, C. H., Sánchez Meador, A. J., Fulé, P. Z., Iniguez, J. M., Baggett, L. S., Fornwalt, P. J., & Battaglia, M. A. (2017). Spatial patterns of ponderosa pine regeneration in high-severity burn patches. *Forest Ecology and Management*, *405*, 134–149.

Pausas, J. G. (2015). Bark thickness and fire regime. *Functional Ecology*, *29*, 315–327.

Pausas, J. G., & Bond, W. J. (2020). Alternative biome states in terrestrial ecosystems. *Trends in Plant Science*, *25*, 250–263.

Pausas, J. G., & Fernández-Muñoz, S. (2012). Fire regime changes in the Western Mediterranean Basin: From fuel-limited to drought-driven fire regime. *Climatic Change*, *110*, 215–226.

Pausas, J. G., & Keeley, J. E. (2021). Wildfires and global change. *Frontiers in Ecology and the Environment*, *19*, 387–395.

Pausas, J. G., & Paula, S. (2012). Fuel shapes the fire–climate relationship: Evidence from Mediterranean ecosystems. *Global Ecology and Biogeography*, *21*, 1074–1082.

Pausas, J. G., & Ribeiro, E. (2013). The global fire–productivity relationship. *Global Ecology and Biogeography*, *22*, 728–736.

Pausas, J. G., & Ribeiro, E. (2017). Fire and plant diversity at the global scale. *Global Ecology and Biogeography*, *26*, 889–897.

Piñol, J., Beven, K., & Viegas, D. X. (2005). Modelling the effect of fire-exclusion and prescribed fire on wildfire size in Mediterranean ecosystems. *Ecological Modelling*, *183*, 397–409.

Ponisio, L. C., Wilkin, K., M'Gonigle, L. K., Kulhanek, K., Cook, L., Thorp, R., Griswold, T., & Kremen, C. (2016). Pyrodiversity begets plant–pollinator community diversity. *Global Change Biology*, *22*, 1794–1808.

Reisen, F., Duran, S. M., Flannigan, M., Elliott, C., Rideout, K., Reisen, F., Duran, S. M., Flannigan, M., Elliott, C., & Rideout, K. (2015). Wildfire smoke and public health risk. *International Journal of Wildland Fire*, *24*, 1029–1044.

Rogers, B. M., Soja, A. J., Goulden, M. L., & Randerson, J. T. (2015). Influence of tree species on continental differences in boreal fires and climate feedbacks. *Nature Geoscience*, *8*, 228–234.

Sannikov, S. N., & Goldammer, J. G. (1996). In J. G. Goldammer & V. V. Furyaev (Eds.), *Fire ecology of pine forests of northern Eurasia. Fire in ecosystems of boreal Eurasia forestry sciences* (pp. 151–167). Springer.

Sauquet, H., Weston, P. H., Anderson, C. L., Barker, N. P., Cantrill, D. J., Mast, A. R., & Savolainen, V. (2009). Contrasted patterns of hyperdiversification in Mediterranean hotspots. *Proceedings of the National Academy of Sciences*, *106*, 221–226.

Schroeder, W., Csiszar, I., & Morisette, J. (2008). Quantifying the impact of cloud obscuration on remote sensing of active fires in the Brazilian Amazon. *Remote Sensing of Environment*, *112*, 456–470.

Smith, J. R., Letten, A. D., Ke, P.-J., Anderson, C. B., Hendershot, J. N., Dhami, M. K., Dlott, G. A., Grainger, T. N., Howard, M. E., Morrison, B. M. L., Routh, D., San Juan, P. A., Mooney, H. A., Mordecai, E. A., Crowther, T. W., & Daily, G. C. (2018). A global test of ecoregions. *Nature Ecology & Evolution*, *2*, 1889–1896.

Syphard, A. D., & Keeley, J. E. (2020). Mapping fire regime ecoregions in California. *International Journal of Wildland Fire*, *29*, 595–601.

Syphard, A. D., Keeley, J. E., Pfaff, A. H., & Ferschweiler, K. (2017). Human presence diminishes the importance of climate in driving fire activity across the United States. *Proceedings of the National Academy of Sciences*, *114*, 13750–13755.

Turetsky, M. R., Kane, E. S., Harden, J. W., Ottmar, R. D., Manies, K. L., Hoy, E., & Kasischke, E. S. (2011). Recent acceleration of biomass burning and carbon losses in Alaskan forests and peatlands. *Nature Geoscience*, *4*, 27–31.

van der Werf, G. R., Randerson, J. T., Giglio, L., Gobron, N., & Dolman, A. J. (2008). Climate controls on the variability of fires in the tropics and subtropics. *Global Biogeochemical Cycles*, *22*, GB3028.

Verdú, M., & Pausas, J. G. (2007). Fire drives phylogenetic clustering in Mediterranean Basin woody plant communities. *Journal of Ecology*, *95*, 1316–1323.

Westerling, A. L., Hidalgo, H. G., Cayan, D. R., & Swetnam, T. W. (2006). Warming and earlier spring increase western US forest wildfire activity. *Science*, *313*, 940–943.

Wood, S. N. (2017). *Generalized additive models: An introduction with R* (2nd ed.). Chapman and Hall/CRC.

Zimov, S. A., Chuprynin, V. I., Oreshko, A. P., Chapin, F. S., III, Reynolds, J. F., & Chapin, M. C. (1995). Steppe-tundra transition: A herbivore-driven biome shift at the end of the Pleistocene. *American Naturalist*, *146*, 765–794.

BIOSKETCH

Juli G. Pausas is a research ecologist of the Spanish National Research Council (CSIC, Spain). His research focuses on the ecology and evolution of disturbance-prone ecosystems and, specifically, on understanding the role of fire in shaping species, populations, communities, landscapes and biomes.

SUPPORTING INFORMATION

Additional supporting information can be found online in the Supporting Information section at the end of this article.

How to cite this article: Pausas, J. G. (2022). Pyrogeography across the western Palaearctic: A diversity of fire regimes. *Global Ecology and Biogeography*, *00*, 1–10. https://doi.org/10.1111/geb.13569

Supplementary Information

Pausas J.G. Pyrogeography across the western Palearctic: a diversity of fire regimes. *Global Ecology & Biogeography*, doi:10.1111/geb.13569

Contents

Table S1. Brief description of the eight regions with different environments considered in western Eurasia. WWF ecoregions codes are from Dinerstein et al. (2017); each ecoregion is fully included in a single region. Countries are indicated by their official codes (ISO Alpha-2) followed by the proportion of the country within the regions (rounded, i.e., 0 refers to < 0.5%).

Region	Extension (km^2)	Description
Mediterranean	2,091,232	Evergreen forest and shrublands around the Mediterranean sea, with Mediterranean climate *WWF Ecoregions*: 644, 701, 758, 785, 786, 788, 789, 790, 791, 792, 793, 794, 795, 796, 797, 798, 799, 800, 801, 802, 803, 804, 805, 806. *Countries*: AL 90, BA 9, BG 0, CY 98, DZ 13, EG 0, EH 1, ES 84, FR 12, GI 69, GR 88, HR 24, IL 39, IQ 0, IT 68, JO 8, LB 99, LY 4, MA 78, MC 100, ME 31, MK 22, MT 75, PS 81, PT 80, SA 0, SI 7, SM 100, SY 27, TN 53, TR 34, VA 100, XK 2
Arid	10,597,943	North Africa (excluding the northernmost part, with Mediterranean climate) and the Arabian Peninsula. Arid climate; the driest region *WWF Ecoregions*: 722, 723, 739, 744, 745, 747, 787, 809, 810, 811, 821, 822, 830, 831, 832, 833, 836, 837, 839, 840, 842, 844, 845, 846 *Countries*: AE 99, BH 84, DZ 85, EG 99, EH 99, ES 1, IL 60, IQ 91, IR 1, JO 92, KW 97, LY 96, MA 22, ML 34, MR 54, NE 44, OM 98, PS 19, QA 98, SA 95, SD 29, SY 73, TD 31, TN 47, TR 0, YE 70
Atlantic	915,465	The west most, including British Islands, temperate with Atlantic (rainy) climate *WWF Ecoregions*: 647, 648, 651, 663, 664, 672, 691, 729, *Countries*: BE 74, DE 30, DK 92, ES 12, FO 86, FR 46, GB 98, GG 64, IE 98, IM 93, JE 81, NL 97, PL 14, PT 16, SE 2
Mountains	737,196	Discontinuous region that include Eurasian high mountains (Alps, Pyrenees, Urals …). Mountain coniferous forests and above treeline. Cold climate *WWF Ecoregions*: 650, 660, 676, 678, 689, 692, 719, *Countries*: AD 100, AL 7, AM 52, AT 58, AZ 30, BA 54, BG 25, CH 56, CZ 2, DE 1, ES 3, FR 6, GE 73, GR 1, HR 20, IT 18, LI 71, ME 68, MK 5, PL 6, RO 23, RS 4, RU 1, SI 43, SK 36, TR 3, UA 6, XK 4
Boreal	2,262,366	North European boreal (coniferous) forests; cold climate *WWF Ecoregions*: 717, *Countries*: FI 97, NO 30, RU 9, SE 58
Steppes	1,336,754	The east part, Black sea and Anatolian forest and steppes (dry/cold grasslands), with continental climate. *WWF Ecoregions*: 652, 658, 662, 703, 725, 735, *Countries*: BG 0, KZ 3, MD 23, RO 10, RU 4, TR 40, UA 41
Continental	3,457,712	Mix forest and moist grasslands in the central part of Western Eurasia. Cold temperate climate *WWF Ecoregions*: 646, 654, 661, 665, 674, 675, 679, 686. *Countries*: AL 2, AT 42, AX 61, BA 37, BE 26, BG 74, BY 100, CH 44, CZ 98, DE 68, EE 98, FI 1, FR 36, GE 9, GR 8, HR 54, HU 100, IT 14, LI 29, LT 100, LU 100, LV 100, MD 77, ME 1, MK 73, NL 0, NO 3, PL 80, RO 67, RS 96, RU 6, SE 27, SI 50, SK 64, TR 11, UA 52, XK 94

Tundra	590,337	The top north with tundra (non-forested) vegetation. The coldest. *WWF Ecoregions*: 774, 776, 780. *Countries*: FI 1, NO 58, RU 2, SE 11
TOTAL	21,896,929	81 WWF ecoregions; 78 countries

Table S2. Average climatic variables for each of the ecoregions considered. For each variable, the highest and lowest are indicated in **bold** and *italics*, respectively. Temperature (temp) is ºC, prcipitation in mm.

	Mediterranean	Arid	Mountains	Atlantic	Boreal	Steppic	Continental	Tundra
Annual mean temperature	14.91	**24.17**	5.10	9.35	1.33	9.04	7.15	*-1.95*
Temp seasonality (sd x 100)	638.9	660.75	832.29	*474.81*	936.73	**952.92**	868.77	862.69
Max temp warmest month	30.36	**39.55**	22.11	20.27	19.59	28.14	23.99	*14.86*
Min temp of coldest month	2.42	**7.99**	-9.89	0.77	-14.86	-7.65	-7.87	*-16.39*
Temperature annual range	27.94	31.56	32.00	*19.5*	34.45	**35.79**	31.86	31.26
Mean temp of wettest quarter	10.45	**21.9**	10.97	8.47	11.19	11.88	15.2	*6.61*
Mean temp of driest quarter	22.13	**27.14**	0.25	9.35	-4.85	8.46	0.41	*-6.92*
Mean temp of warmest quarter	22.97	**31.73**	15.35	15.36	13.14	20.52	17.69	*9.17*
Mean temp of coldest quarter	7.44	**15.65**	-5.04	3.86	-10.00	-2.75	-3.57	*-11.83*
Annual precipitation	575.63	*78*	870.96	**1038.79**	666.45	503.64	673.47	675.13
Precipitation of wettest month	88.38	*18.99*	109.68	**118.84**	84.03	66.25	85.13	84.57
Precipitation of driest month	12.09	*0.38*	43.81	**53.89**	32.02	21.21	34.49	33.21
Precipitation seasonality (CV)	**56.01**	76.92	30.85	*24.05*	31.83	34.06	29.8	30.66
Precipitation of driest quarter	50.92	*2.48*	149.12	**177.63**	106.06	72.51	114.73	109.55

Table S3. Source of data for estimating the different fire regime parameters

Fire regime parameter	Source[1]	Period[2]	Scale	Comments
Number of fires	GlobFire	2001-2019	Fire	Fig. S2
	FRY MODIS	2000-2017	Fire	Fig. S2
	GFA	9/2002-4/2017	Fire	Fig. S2
Fire size, area burnt	GlobFire	2001-2019	Fire	Fig. 1
	FRY MODIS	2000-2017	Fire	Scenario 3 and 14, Fig. S3-S6
	GFA	9/2002-4/2017	Fire	Fig. S3-S6
Fire intensity	FRY MODIS	2000-2017	Fire	Mean fire radiative power (megawatts/pixel), Fig. S7-S8
	MODIS hotspots	11/2000-1/2021	Pixel	Fire radiative power (megawatts), for Terra and for Aqua satellites; Fig. 1, S7-S8; spatial resolution: 1 km
Fire season	GlobFire	2001-2019	Fire	Fig. 1
	GFA	9/2002-4/2017	Fire	Fig. S10
	FRY MODIS	2000-2017		Fig. S10
	MODIS hotspots		Fire	Fig. S10
Fire patchiness	FRY MODIS	2000-2017	Fire	CV of fire intensity (radiative power). Scenario 3 and 14, Fig. S9
Fire recurrence	GlobFire	2001-2019	Patch	Fig. 1; patch obtained by overlying all fires
Pyrodiversity	GlobFire	2001-2019	Patch	Fig. 1; idem

1) Acronyms: GWIS: Global Wildfire Information System (Artés et al. 2019); GFA: Global Fire Atlas (Andela et al. 2019), FRY MODIS (Laurent et al. 2019), MODIS hotspots (NASA, MCD14ML data obtained from the University of Maryland; data with confidence > 60)
2) Some sources include incomplete years, thus for annual information, only complete years where considered

Table S4. Summary of the statistical of the smooth fitting in Fig. 2 (main text) using generalised additive models.

Fire (dependent) variable	Climate (independent) variable	ΔAIC	F	P-val	R^2 adj	Dev. Expl. (%)
Fire size	Mean temperature of the driest quarter	8.85	8.118	0.0292	0.504	57.5
Fire intensity	Mean temperature of the driest quarter	5.93	5.44	0.0396	0.579	66.1
Fire patchiness	Mean temperature of the wettest quarter	14.46	21.61	0.0033	0.860	90.0
Fire recurrence	Mean temperature of the driest quarter	7.17	12.88	0.0115	0.629	68.2

Table S5. Skewness and Pearson's kurtosis of fire size and intensity based on FRY, for scenarios. Extreme low fire intensity values (mean = $4 \cdot 10^{-7}$) are excluded. Values in bold indicate the ecoregion with the highest vaule for each column.

	Modis, scenario= 03				Modis, scenario =14			
	Fire size		Mean fire intensity		Fire size		Mean fire intensity	
Ecoregion	Skewness	Kurtosis	Skewness	Kurtosis	Skewness	Kurtosis	Skewness	Kurtosis
Mediterranean	19.29	530.13	6.56	82.55	18.04	471.61	6.49	80.51
Arid	26.53	1111.41	5.54	59.62	18.03	470.18	4.25	30.47
Mountains	15.49	447.57	5.62	62.35	8.45	130.72	6.16	80.39
Atlantic	12.72	276.01	3.61	21.98	10.85	191.94	**6.76**	**97.49**
Boreal	35.46	1496.27	3.85	30.48	33.97	1443.20	3.70	27.30
Steppes	54.76	4225.45	5.90	72.37	54.59	4157.05	6.41	87.54
Continental	**62.34**	**6718.75**	**6.98**	**109.86**	**71.15**	**9579.49**	6.42	84.54
Tundra	1.38	3.66	0.43	2.33	1.05	2.68	0.25	1.91
Overall	64.76	6430.67	7.09	110.15	61.73	5835.59	7.45	122.35

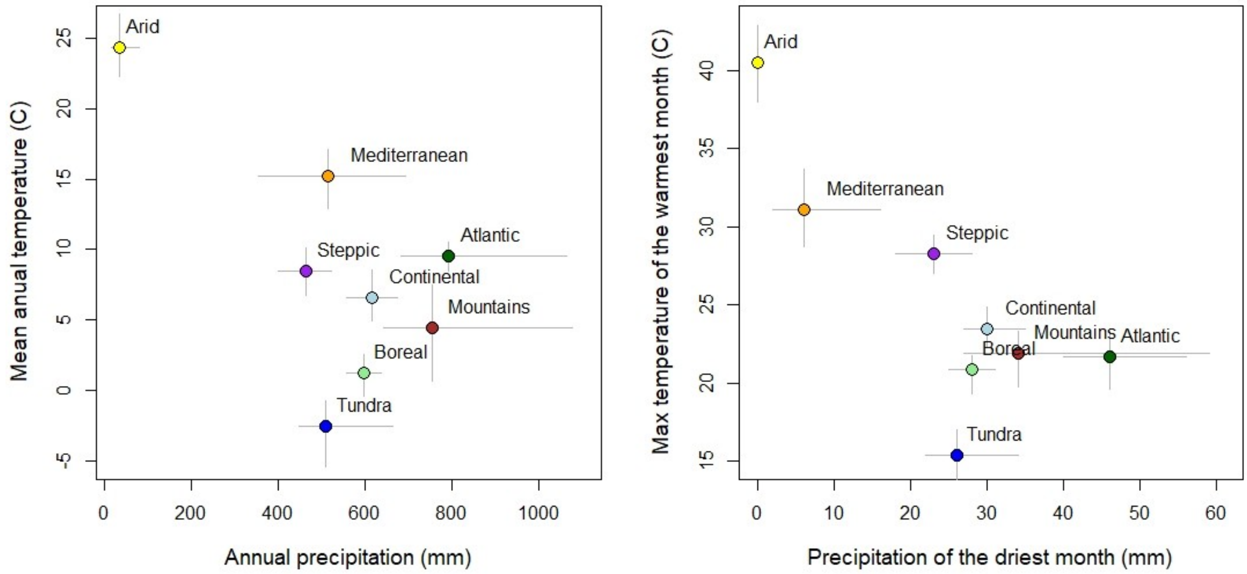

Fig. S1. Distribution of the ecoregions in the environmental space defined by mean annual temperature (y axis, ºC) and annual rainfall (x axis, mm) (left), and by maximum temperature of the warmest month and precipitation of the driest month (x axis, mm) (right). Colored symbols are the media, and lines are the 25% and 75% percentiles (spatial variability).

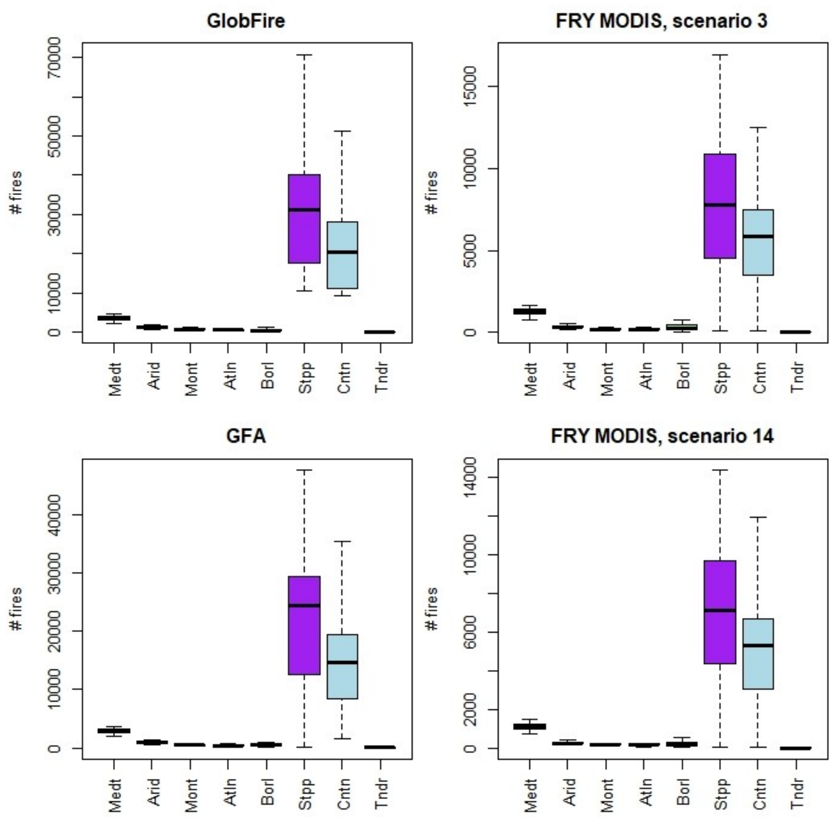

Fig. S2. Mean annual number of fires. Variability refers to different years. Scenarios 3 and 14 refers to the 3 and 14 days cutoff following Laurent et al. 2018, 2019.

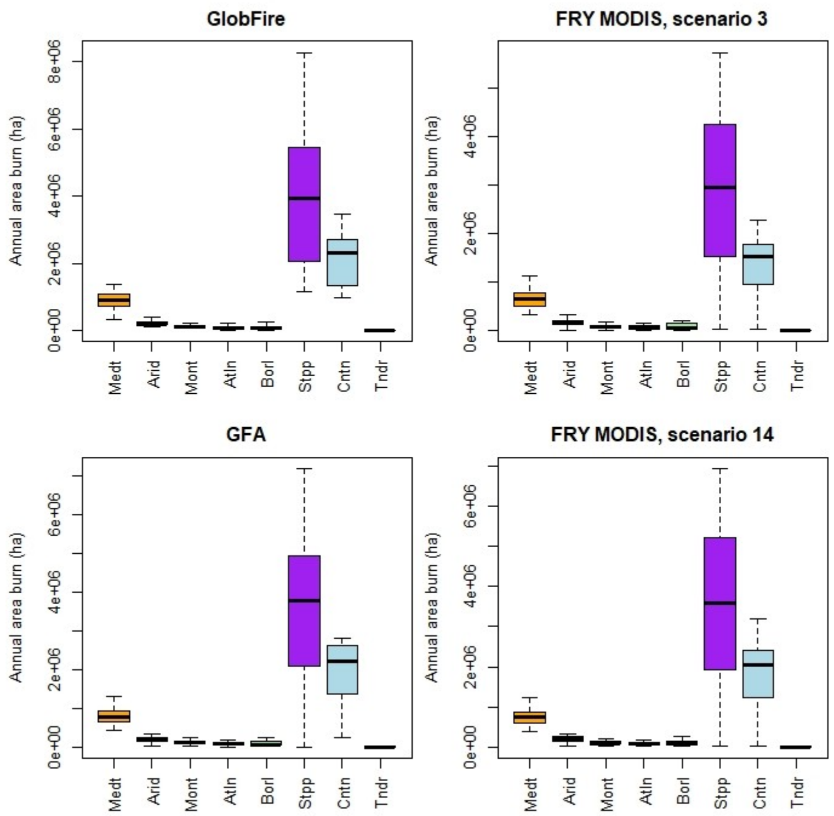

Fig. S3. Annual area burnt. Variability refers to different years. Scenarios 3 and 14 refers to the 3 and 14 days cutoff following Laurent et al. 2018, 2019.

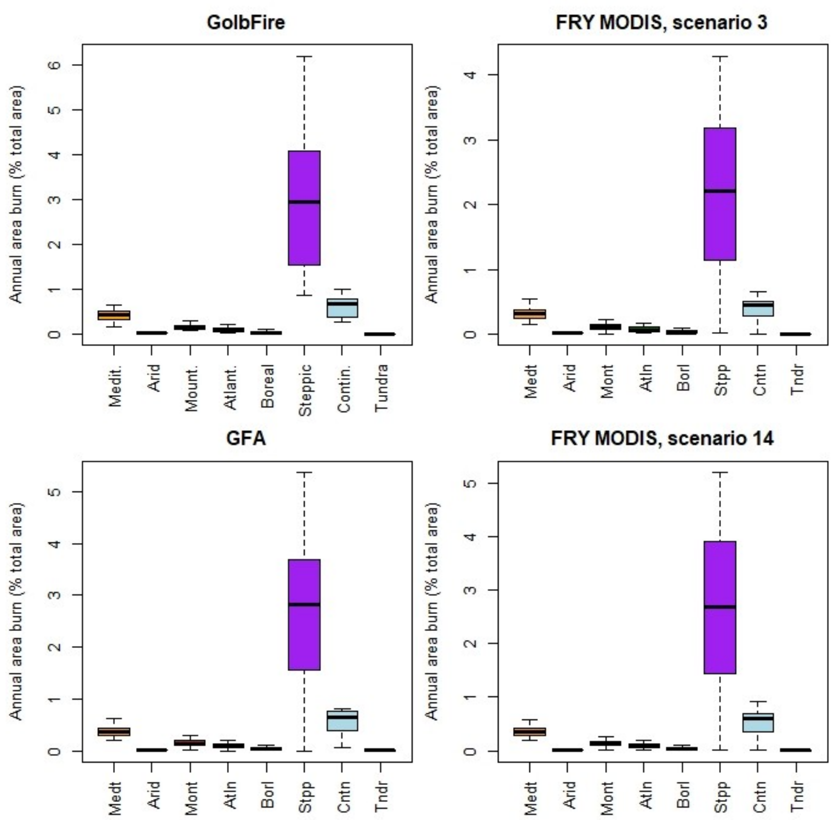

Fig. S4. Relative annual area burnt (in relation to the size of the region)

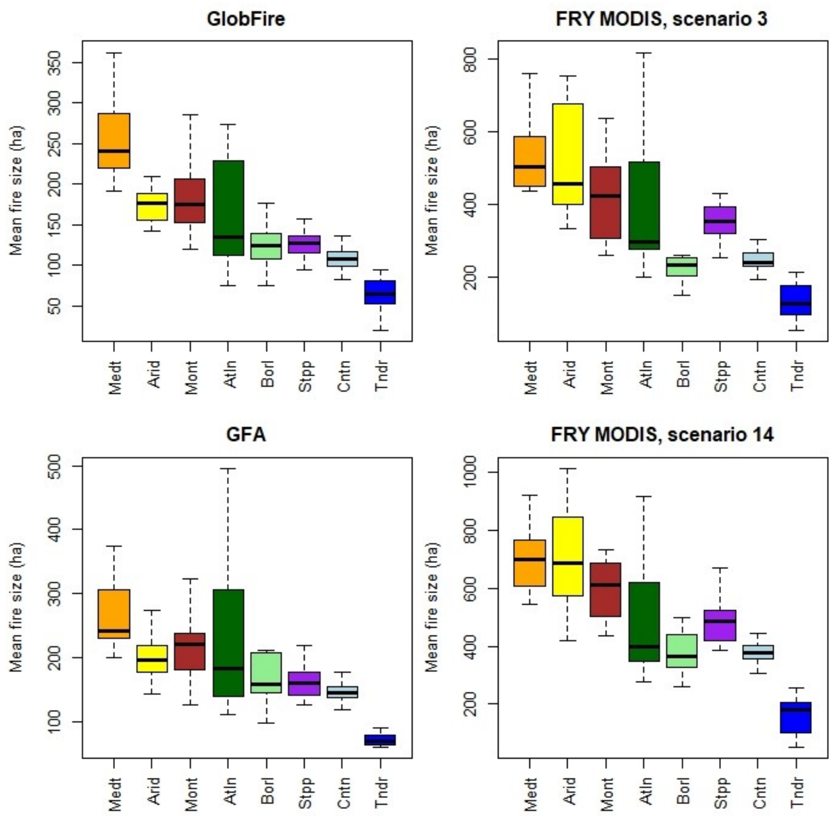

Fig. S5. Mean fire size

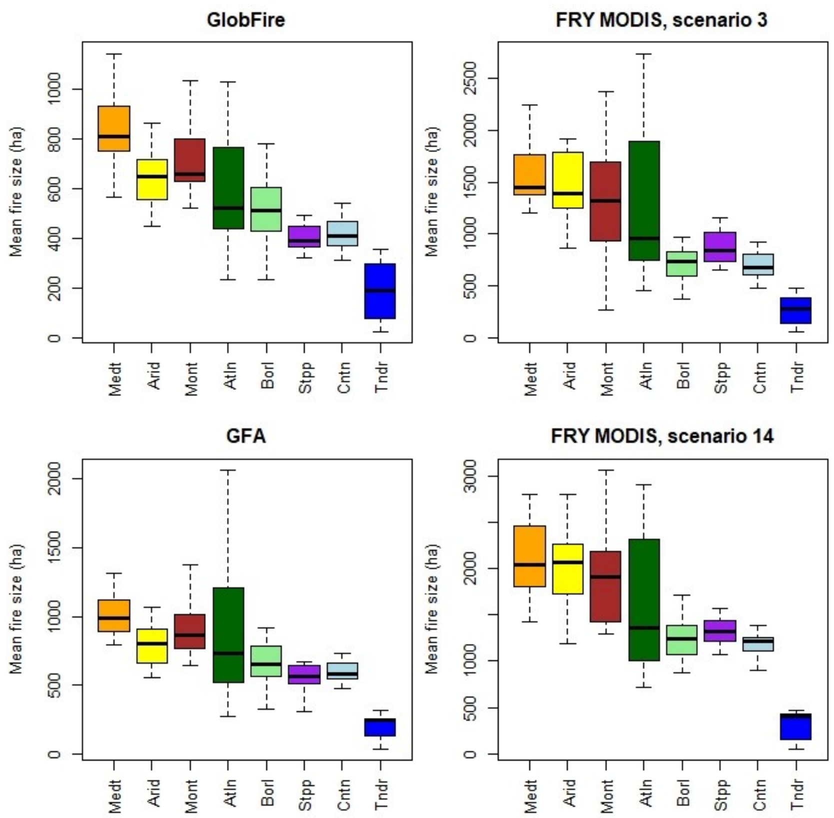

Fig. S6. Max fire size (percentile 95%)

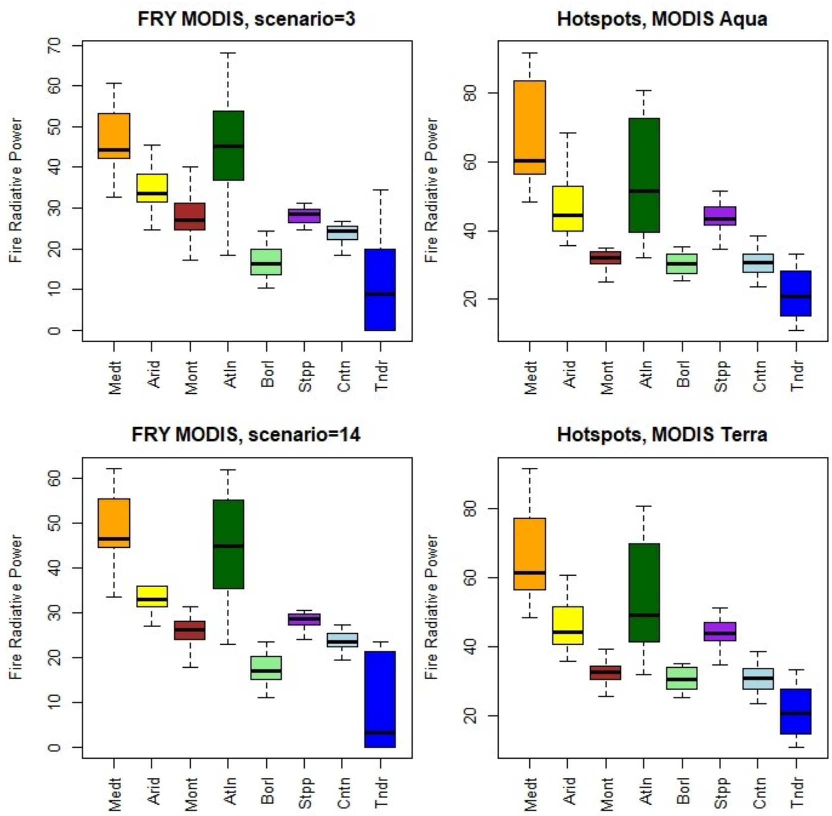

Fig. S7. Fire intensity as mean fire radiative power (left), and pixel fire intensity (left).

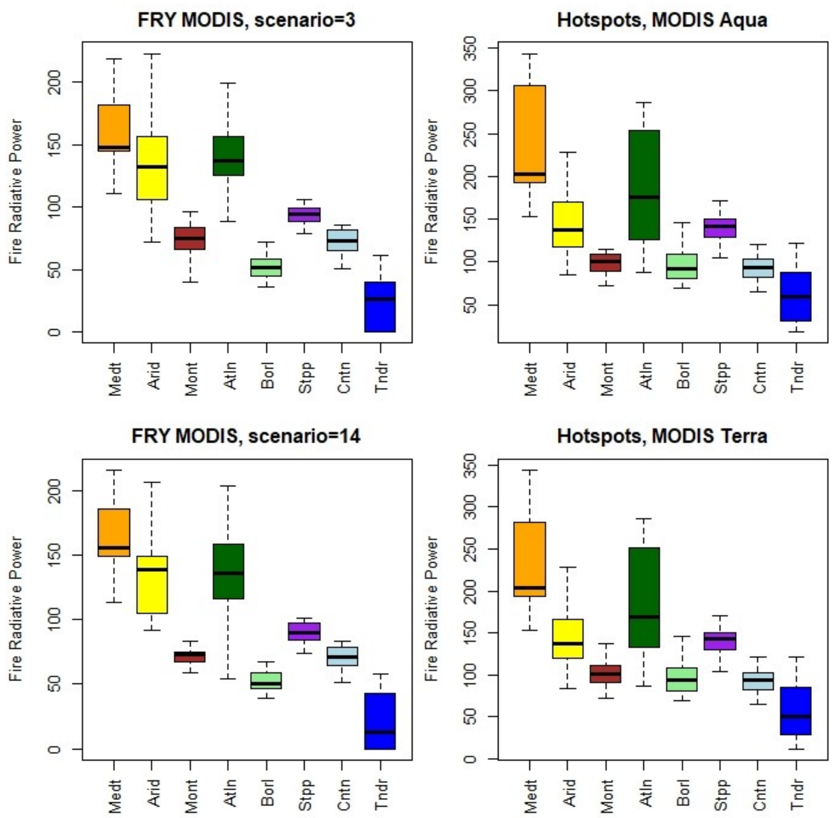

Fig. S8. Maximum fire intensity as 95% quantile of fire radiative power (left), and pixel fire intensity (left).

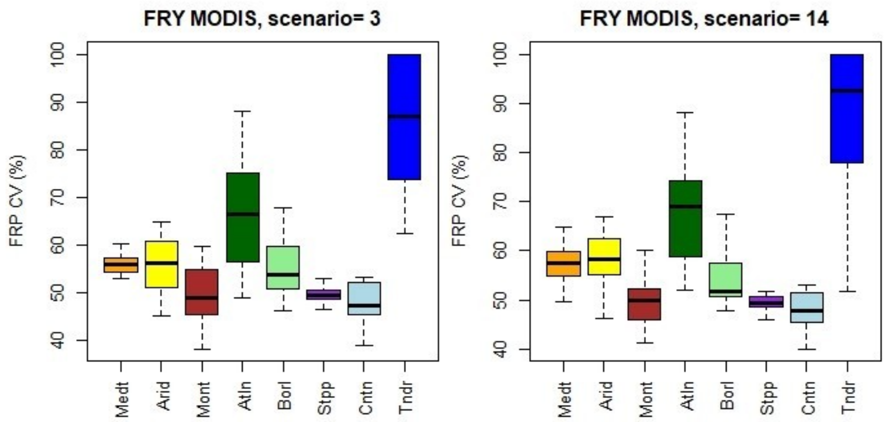

Fig. S9. Indicators of fire patchiness: coefficient of variation of the fire radiative power (FRP) within a fire. The most patchy fires occur in the Tundra.

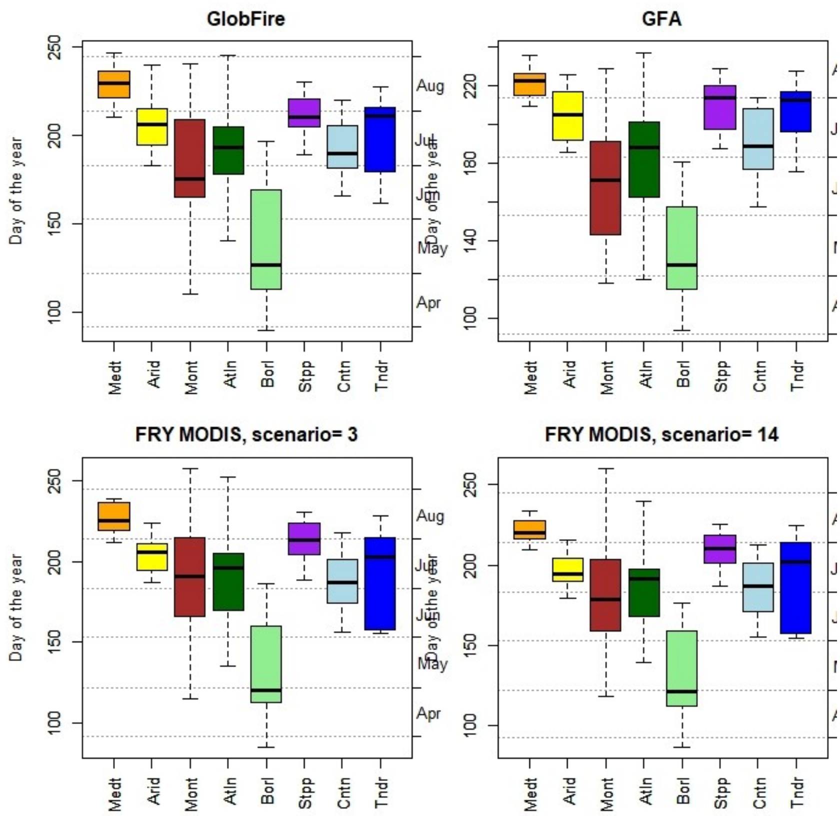

Fig. S10. Fire season

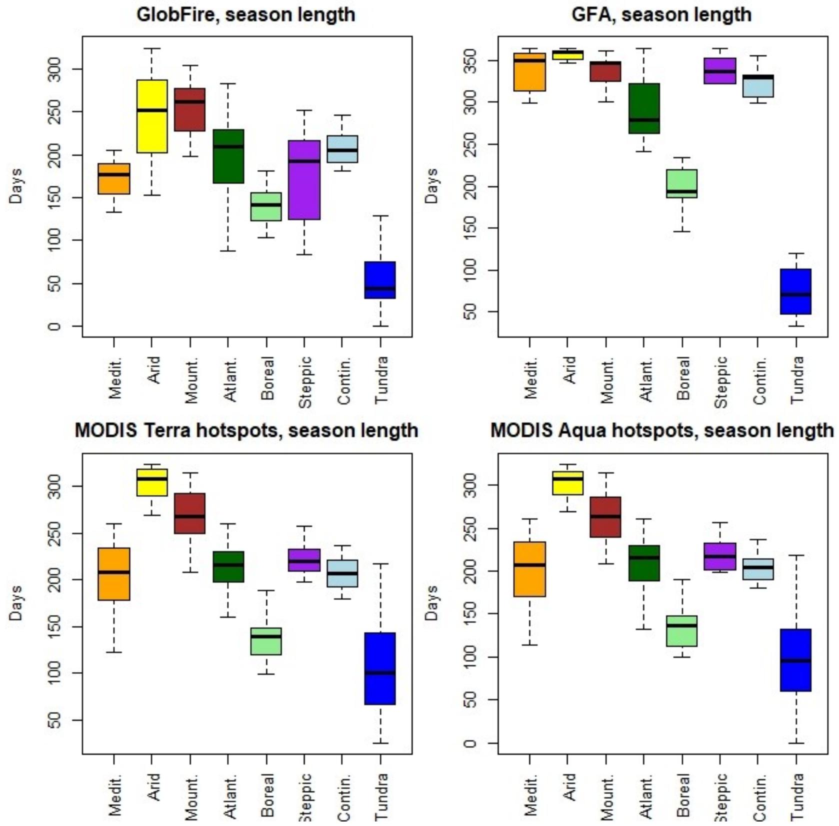

Fig. S11. Duration of the fire season calculated as the number of days between the 0.05 and the 0.95 percentiles of the first and last fire (GlobFire, GFA) or hotspot (MODIS) of each year.

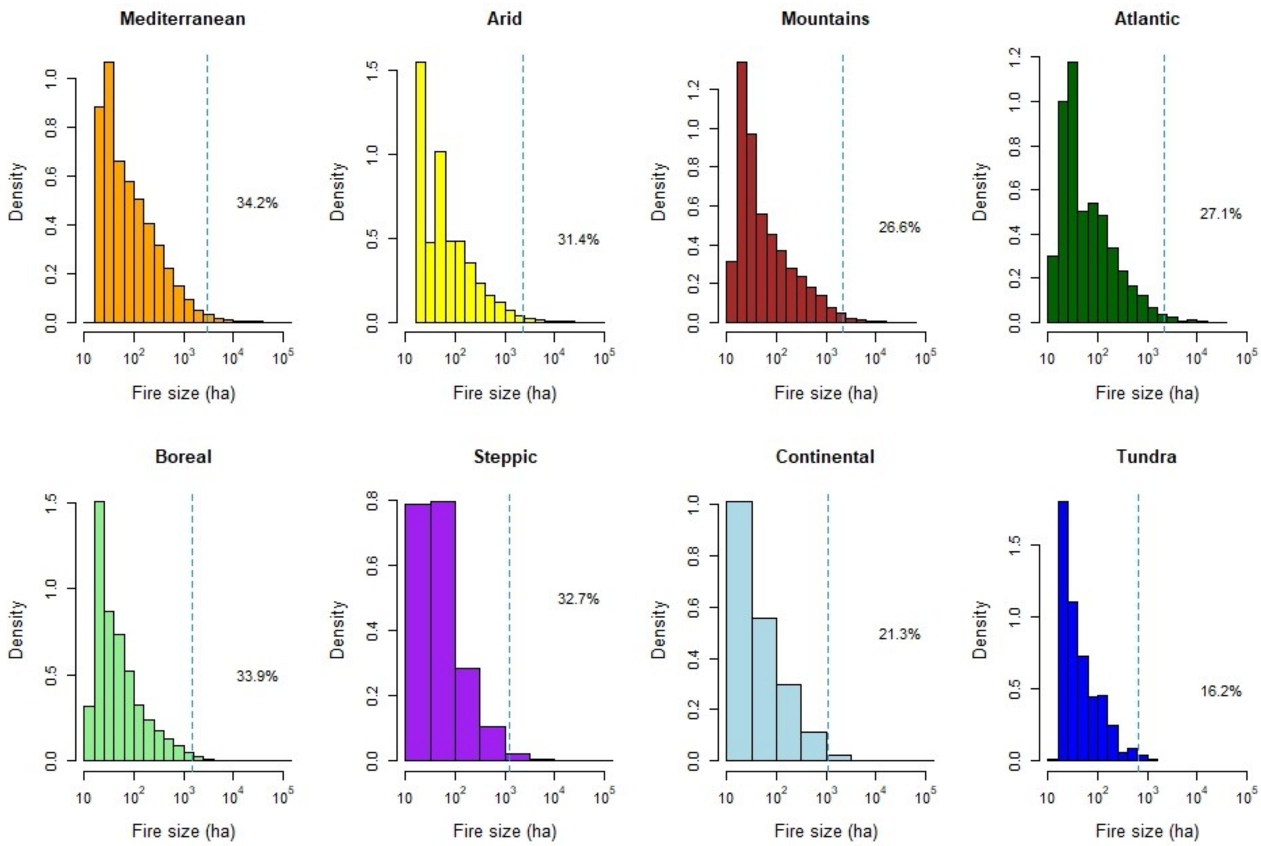

Fig. S12. Fire size distribution for the eight ecoregions in the western Palearctic. Vertical dotted lines indicate the percentile 99%, and the number in the right of the line is the proportion of the area burned by the top 1% fires. This value for the entire regions is 30% (see Fig. S15).

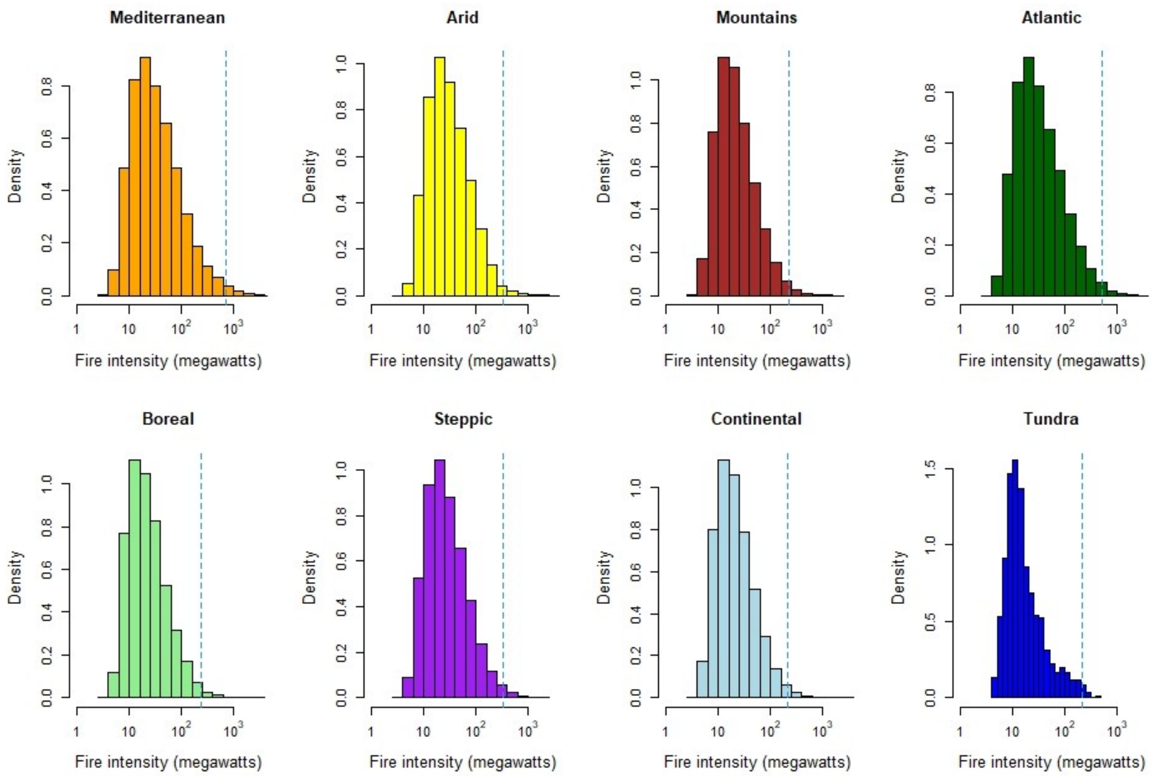

Fig. S13. Frequency distribution of fire intensity (pixel scale, Table S2) for the eight ecoregions in the western Palearctic. Vertical dotted lines indicate the percentile 99%.

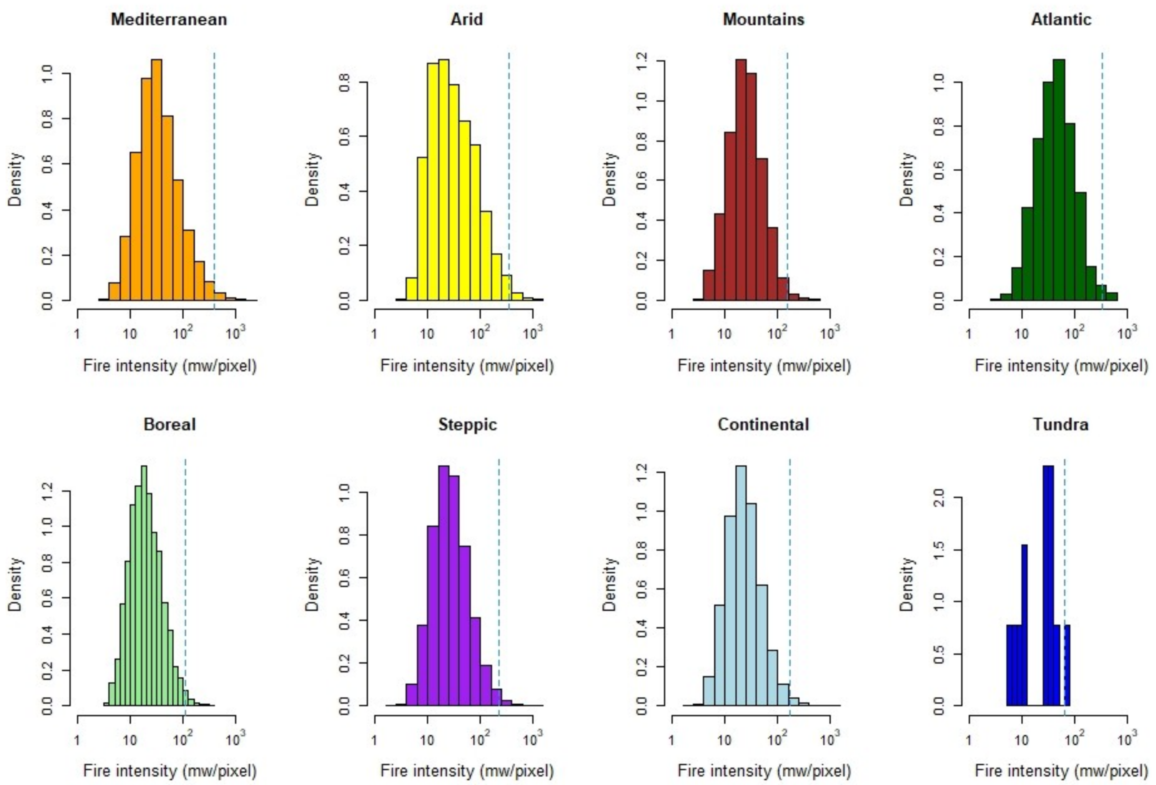

Fig. S14. Frequency distribution of fire intensity (fire scale; from FRY, see Table S2) for the eight ecoregions in the western Palearctic. Vertical dotted lines indicate the percentile 99%.

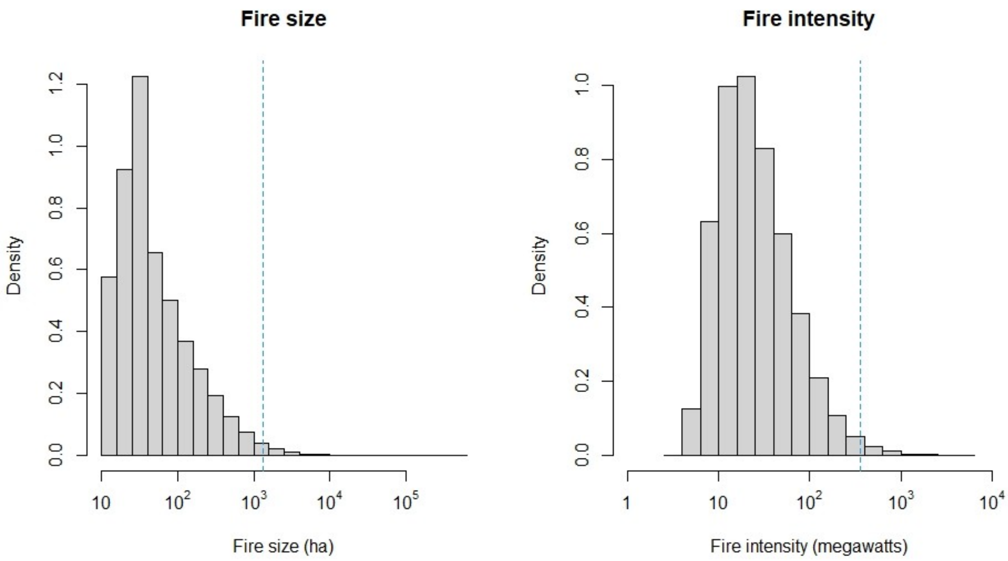

Fig. S15. Frequency distribution of fire size (left) and fire intensity (right; hotspots, pixel scale) for the whole study area (western Palearctic). Vertical lines indicate the 99% percentile.

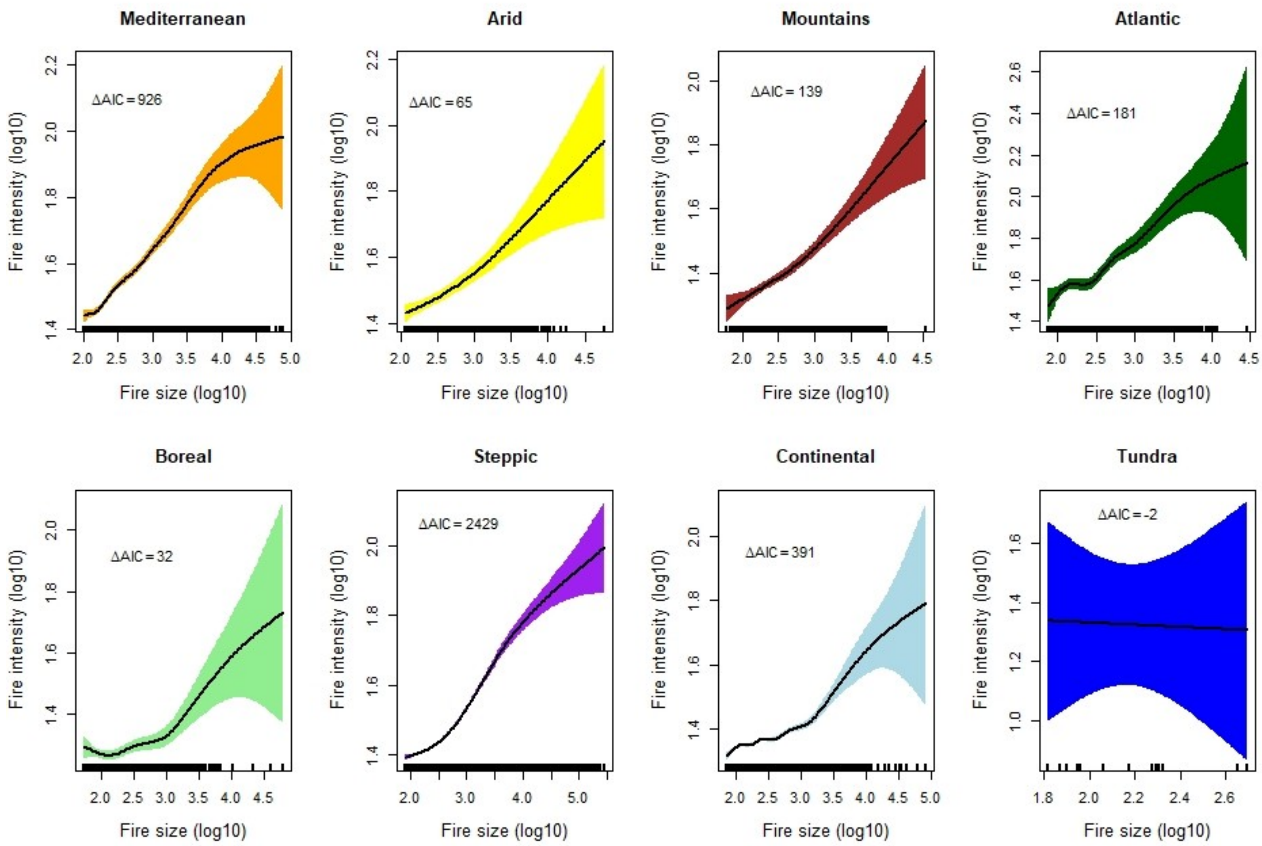

Fig. S16. Relationship between fire size and fire intensity (mean fire radiative power) for the different regions considered. The figure shows the smoothing (generalized additive model) and the AIC change after fitting the model (note that for Tundra is negative, i.e., non-significant). Shade areas are confidence intervals. The two axes are in log-scale. Data from FRY.

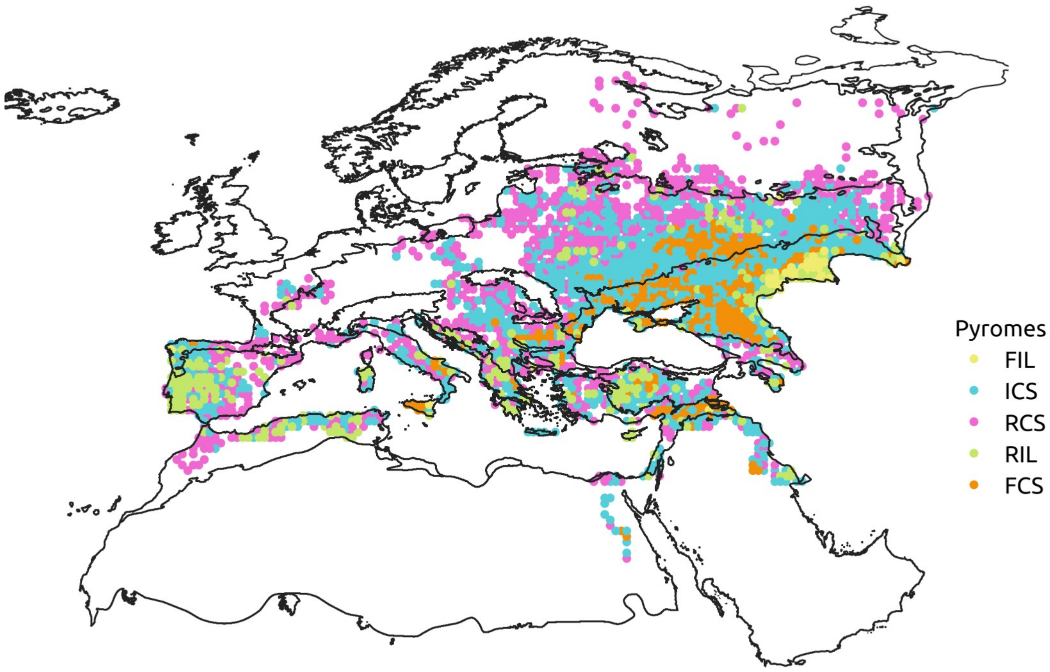

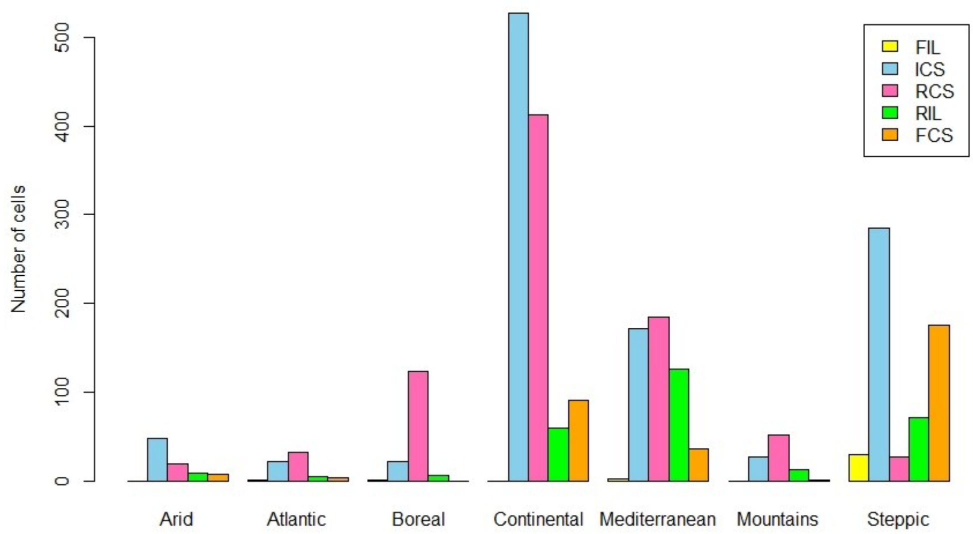

Fig. S17. Map of pyromes for the study area from Archibald et al. (2013) (top) and number of cells (pixels) for each pyrome in each of the regions considered (bottom). Note that there were no pixels with pyrome information in the Tundra, so it is not shown in the bottom figure. Abbreviations as in Archibald et al. (2013): FIL (frequent–intense–large), ICS (intermediate–cool–small), RCS (rare–cool–small), RIL (rare–intense–large), and FCS (frequent–cool–small).